

add-10

AD655634

TNO

MECHANICAL PROPERTIES OF HIGHLY FILLED ELASTOMERS VI.

Influence of filler content and temperature on
ultimate tensile properties.

Reported by

C.J. Nederveen and H.W. Bree

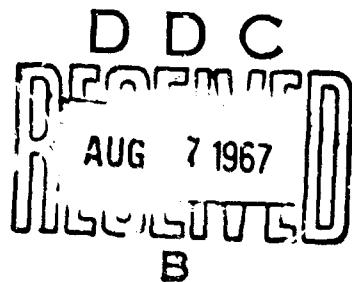
CENTRAAL
LABORATORIUM

T.N.O.

RECEIVED

AUG 8 1967

CFSTI



**Best
Available
Copy**



MECHANICAL PROPERTIES OF HIGHLY FILLED ELASTOMERS VI.

Influence of filler content and temperature on
ultimate tensile properties.

Reported by

C.J. Nederveen and H.W. Bree

132 JULIANALAAN · DELFT · TELEPHONE 01730-37000 · THE NETHERLANDS

CENTRAL LABORATORY TNO

ONR Technical Report No. 6

Mechanical Properties of Highly Filled Elastomers VI.

Influence of filler content and temperature on
ultimate tensile properties

by

C.J. Nederveen and H.W. Bree

Contribution from the Central Laboratory TNO
Delft, Netherlands.

Report No. CL 67/34

Contract No. N 62558-4375

Distribution of this document
is unlimited

Delft, May 1967

MECHANICAL PROPERTIES OF HIGHLY FILLED ELASTOMERS VI.

Influence of filler content and temperature on ultimate tensile properties.

Reported by

C.J. Nederveen and H.W. Bree

The work reported here was carried out by:

H.W. Bree, assisted by Miss M.P. van Duykeren.	Preparation and characterization of filled polyurethanes.
C.J. Nederveen, assisted by J. Wesselius.	Measurement of tensile properties of filled rubbers.
G.A. Schrippert and C.W. v.d. Wal.	Digital read-out and processing of measuring data.
R. Nauta, assisted by G.J. Kap.	Machining of specimens.
B. de Goede (Central Technical Institute TNO).	Classification of filler substance.

CONTENTS.

SUMMARY.

1. INTRODUCTION.
2. MATERIALS.
3. EXPERIMENTAL TECHNIQUE.
4. DISCUSSION OF RESULTS.
 - 4.1. Stress-strain data.
 - 4.2. Modulus of elasticity.
 - 4.3. Failure envelope.
 - 4.4. Dewetting.
 - 4.5. Comparison with results of tensile creep measurements.
5. CONCLUSIONS.
6. REFERENCES.

TABLE.

CAPTIONS TO FIGURES.

FIGURES.

DISTRIBUTION LIST

SUMMARY.

Results are presented of stress-strain tests performed at various temperatures and strain rates on materials filled with various amounts of sodium chloride particles with a mean size of 0.1 mm. Stress and strain at rupture decreased with increasing filler content. For each material investigated it was possible to construct the well-known failure envelope by means of which the results could be described adequately.

The dewetting of the particles in the rubbery matrix, sometimes resulting in a maximum in the stress-strain curve, is ascribed to failure of the rubber between the particles and not to failure of the rubber-salt bond, because the dewetting maximum was dependent on temperature and time in the same way as the rupture properties of the unfilled material.

The results are compared with earlier investigations, e.g. high speed tensile tests and creep experiments, and a good agreement is found.

1. INTRODUCTION.

In the design of solid rocket motors, a thorough knowledge of the mechanical behaviour of solid propellant grains is very important. We especially mention the formation of cracks in the propellant, which leads to malfunction of the motor. Cracks may be formed during storage; they are then due to shrinkage or thermal stresses. Or during combustion, when they are due to combustion pressure or acceleration forces.

The composite propellant under study consists of a polyurethane rubber filled with ammonium perchlorate particles. For ease of handling, we have so far used model substances consisting of the same rubber but filled with an inert material, viz. sodium chloride. Various fractions of NaCl were used. The influence of filler size, shape, concentration and surface treatment on the mechanical behaviour of those materials was studied and reported earlier (1 - 8).

The present report describes failure properties of the model materials filled with salt particles of one particular size (about 0.1 mm): tensile tests were performed on dumb-bell-shaped specimens at various temperatures.

2. MATERIALS.

All samples of filled and unfilled polyurethane rubbers investigated were based on a linear (polypropylene ether)glycol (Desmophon 3600, Farben Fabriken Bayer, Leverkusen, Germany) with a molecular weight of about 2000. The molecules of this polyether were lengthened with toluene diisocyanate and crosslinked by means of trimethylol propane in the presence of a catalyst. Full details concerning the preparation of these filled and unfilled rubbers were given previously (1,2,7).

A series of samples was prepared containing various amounts (0, 15, 30 and 45% by volume) of sodium chloride particles of about 100 μm [fraction no. 4 (2), labelled 90-105 μm , with largest dimensions between 50 and 175 μm and smallest dimensions between 25 and 100 μm]. No surfactant was used in the preparation of these materials. In order to provide sufficient material for this study, all compositions were made in sixfold.

Details of each batch are given in Table 1^{*)}. This table contains, for each batch, the chemical composition of the prepolymer; the content of filler, as calculated from the weights of the ingredients used, and as calculated from the density; the fraction number and the size of the filler; the equilibrium swelling ratio (5% vol. increase) in two different solvents (chloroform and trichloroethylene); the density, d . Details of these routine control measurements were given earlier⁽²⁾. The last column of Table 1 gives the temperatures at which stress-strain tests were performed.

From Table 1 it is seen that the chemical composition of the rubbery binder was approximately the same for all samples prepared (columns 2, 3, 4). Columns 5 and 6 show that the differences between the volume concentration as calculated from the weights of the ingredients used and that calculated from the density are smaller than 1.0 vol.-%.

As there exists a distinct relationship between crosslinking density and equilibrium swelling, a constancy of swelling data (columns 10 & 11) indicates a constancy of the cross-linking density.

The materials were stored at 20°C and 65% relative humidity for at least 14 days prior to the machining of test specimens.

*) See page 20.

3. EXPERIMENTAL TECHNIQUE.

Dumb-bell-shaped specimens were machined, on a modified Maximat Standard^{*)}, from the materials described above. Shape and dimensions are given in Fig. 1.

Stress-strain measurements were performed on a tensile testing machine at various cross-head speeds (10, 20, 40 and 60 cm/min), and at various temperatures (-45, -40, -35, -30, -20, 0 and 30°C).

A small tensile tester, developed by the Rubber Research Institute TNO, was kindly placed at our disposal by the said institute. A cabinet was placed around the specimen, including the grips, and thermostated gas was blown into the chamber. For temperatures above ambient, electrically heated air was used. For temperatures below ambient, air was blown along solid CO₂. In the cabinet, a temperature sensor operated an electrical heating device and thus regulated the temperature. The sensor element was calibrated with a thermometer placed in the cabinet.

The tensile force was measured with a force transducer at the upper clamp (the lower clamp was the driven clamp). The electrical output of this transducer was fed to a strip chart recorder. The voltage of the signal was printed digitally at fixed time intervals of 2½ sec. These data were used for evaluation of the results, using a digital computer, afterwards.

The tensile stress, σ , was calculated with respect to the original cross-section of the prismatic part of the specimen.

The tensile strain, ϵ , of the prismatic part of the specimen depends on the displacement, Δl , of the clamps. As the cross-section is not uniform and the material behaves non-Hookean, an exact value for ϵ cannot be obtained from the clamp displacement. A minimum, ϵ_{\min} , is found by assuming the material to be Hookean everywhere, and a maximum, ϵ_{\max} , by assuming that the heads of the specimen do not deform at all:

$$\frac{l_2}{l_1 + (l_2 - l_1) \left(\frac{b_1}{b_2} \right)} \left(\frac{\Delta l}{l_1} \right) < \epsilon < \frac{l_2}{l_1} \left(\frac{\Delta l}{l_2} \right) \quad (1)$$

In this expression, l_1 (see Fig. 1) denotes the length between the grips, b_1 denotes the smallest and b_2 the largest width of the specimen. For l_1 the mean value of l_1 and l_2 is chosen, l_2 is approximately representative for the prismatic part of the specimen.

*) Haier & Co, Halluin, Austria.

Shortly after the start of the experiment, deformations are small, and ϵ will be close to ϵ_{\min} ; near the end of the test the heads show little or no dewetting, so ϵ will be closer to ϵ_{\max} . For convenience, the mean value of ϵ_{\max} and ϵ_{\min} was chosen as representative for ϵ . From the dimensions of the dumb-bell according to Fig. 1 it follows that

$$\epsilon = 1.48 (\Delta l/l_2) \quad (2)$$

However, the real strain may differ up to $\pm 30\%$ from this value.

Using this result, it was found that the four cross-head speeds mentioned earlier correspond to strain rates of respectively 0.025, 0.05, 0.1 and 0.15 s^{-1} . These figures are much smaller than the strain rates at which similar materials, prepared in our laboratory, were tested at Columbia University, New York⁽⁹⁾: 0.37, 2.77, 7.40 and 25.1 s^{-1} . The results of "Columbia" will be compared with our results in the present report.

4. DISCUSSION OF RESULTS.

4.1. Stress-strain data.

A considerable spread ($\pm 30\%$) was observed between the rupture properties of individual specimens from the same batch. An investigation concerning the ultimate stress at $+30^{\circ}\text{C}$ of a number of specimens from various batches revealed that the mean values of about 5 measurements on specimens from one batch were rather close to those of tests of other batches. From this finding it was concluded that the batches are practically identical with respect to their ultimate properties.

Sometimes rupture was observed at one of the ends of the prismatic part of the specimen, indicating that machining of specimens, or the shape of the specimen, needed improvement. Results obtained with these specimens were not rejected, however, because no deviations from the general behaviour were observed.

Representative results of stress-strain measurements at various temperatures are shown in Figs 2, 3, 4 & 5; each diagram relates to one particular filler content. The curves presented in these pictures give representatively selected mean values from about 5 tests. Fig. 2 shows results for the unfilled material. With decreasing temperature, the strain-at-break, ϵ_b , reaches a maximum, whereas the stress-at-break, σ_b , increases continuously. The maximum observed in the stress-strain-curve at -45°C has not yet been explained.

Figs 3, 4 and 5 show results for the filled rubbers. ϵ_b and σ_b depend in the same way on temperature as do the rupture properties of the unfilled material. A definite maximum in the stress occurs at low temperatures for all filled materials. For the 45% filled material, this also shows up at room temperature. This maximum can be attributed to a tearing of the rubber bridges between particles, the so-called dewetting. Because, in these regions, the rubber is strained comparatively more than the specimen as a whole, the dewetting takes place at a comparatively low over-all deformation. This dewetting phenomenon will be discussed in more detail in Section 4.4.

Each of Figures 6 to 12 gives the stress-strain diagrams at one constant temperature for various amounts of filler. Observe that stress as well as deformation at rupture appear to decrease with increasing filler content.

4.2. Modulus of elasticity.

The modulus of elasticity, Young's modulus E , was calculated from the initial slope of the stress-strain curve.

The tensile tester used in our experiments was not entirely suitable for this type of tests: one of the troubles was that perfectly straight clamping was impossible. It was estimated that, because of this inconvenience, the initial slope could be in error up to a factor of two. Despite this the modulus was calculated from the initial slope. This was done according to the formula:

$$E = \sigma(1+\epsilon)/\epsilon \quad (3)$$

In Fig. 13, Young's modulus E is plotted for the four different filler concentrations as a function of temperature (open symbols). The filled symbols are results obtained by tensile creep measurements on the same materials ⁽⁸⁾. Also inserted are results (crosses) of tensile tests at high strain rates carried out at Columbia University on similar materials [⁽⁹⁾, Figs 1 and 9]. Moduli calculated from these results in general appear to be 50 to 100% higher than our results. In view of all the possible errors, and the fact of the differences in the testing speed, this range of agreement is satisfactory.

4.3. Failure envelope.

It is known from the literature ⁽¹⁰⁻¹⁵⁾ on rupture properties of filled and unfilled rubbers that a relationship exists between ϵ_b , σ_b , time to break, t_b , and absolute temperature, T . This relationship is described by a curve in a three-dimensional space. Along the three orthogonal axes are plotted respectively $(273 \sigma_b/T)$, ϵ_b , and the reduced time-to-break, t_b/a_T . Quantity a_T is the well-known time-temperature shift according to the W.L.F.-equation:

$$\log a_T = -c_1(T-T_0)/(c_2+T-T_0) \quad (4)$$

The values for a_T were obtained from torsional pendulum and torsional creep measurements at small deformations. The shift factors for the various temperatures were partly published ⁽⁶⁾, and partly obtained from measurements not yet reported.

Unfilled rubber and materials filled with various amounts of sodium chloride were investigated, as is indicated in Fig. 14 by different symbols. A curve according to Eq.(4) was drawn through the individual points. By trial and error it was found that the best fit was obtained through use of the following constants: $T_0 = -35^\circ\text{C}$, $c_1 = 27.6$, $c_2 = 38^\circ\text{C}$. T_0 was arbitrarily chosen as a reference temperature. The shift can be referred to another temperature, \bar{T}_0 , by replacing the constants in Eq.(4) by new constants \bar{c}_1 and \bar{c}_2 ⁽¹⁶⁾

$$\bar{c}_2 = c_2 + \bar{T}_0 - T_0$$

$$\bar{c}_1 = c_1 c_2 / \bar{c}_2$$

(5)

When the glass-transition is taken as a reference, we find that $\bar{T}_0 = T_g = -52^\circ\text{C}$ ⁽⁶⁾, $\bar{c}_1 = 21$, $\bar{c}_2 = 50^\circ\text{C}$. Above 0°C no values for the shift factor a_T were available; according to Williams, Landel and Ferry ⁽¹⁰⁾, the equation for the shift factor holds up to 100°C above T_g . As a consequence, an extrapolation up to -40°C should be justified.

When the curve mentioned before, representing the relationship between ϵ_b , σ_b , t_b and T , is projected onto the σ_b , ϵ_b -plane we obtain the so-called failure-envelope. This is shown for the four materials under investigation in Fig. 15. A rather large spread is observed, but this is not unusual for this type of investigations ⁽¹¹⁾. Fig. 16 gives the upper part of the failure-envelope, in which different symbol fillings are used for the four different temperatures in order to show each temperature dependence. The impression is that measurements belonging to one temperature lie on straight lines making a fixed slope, around unity, with the axis. This may be explained as follows. Each stress-strain curve makes a slope of around unity near the rupture point and the stress-strain curves of all experiments are very much alike. Rupture occurs at various positions along this curve, resulting in the observed scatter. For increasing filler content, the stress-strain curves become more horizontal at their end and the rupture points lie more on a horizontal line.

The two other projections of the curve are shown in Figs 17 and 18. According to Eq.(4), time and temperature are interrelated. Therefore, the horizontal scale in Figs 17 and 18 is at the same time a scale for a reduced temperature. The time-temperature relationship is not a simple expression; for reasons of simplicity we only indicated at the horizontal axis the temperature for a rupture-time of 60 seconds. As in our measurements the variations in strain rate were rather small, points referring to the same temperature tend to cluster.

It was mentioned earlier that shape and level of the curves show a spread of about 30%. As can be seen from Fig. 18, materials with 0 and 45% filler differ a factor of 2 to 10 in rupture strain. The magnitude of this effect is well beyond the experimental spread. It may be concluded that the deformation at rupture decreases with increasing filler content.

The stress-at-break, σ_b , is not subject to geometrical errors. Comparing the 0% and 45% filled materials, we observe a decrease of a factor of 5 at low and a factor of 2.5 at high temperatures. The highest value for the unfilled material is $5 \times 10^7 \text{ N/m}^2$. This value is in accordance with corresponding values given in the literature: $\sigma_b = 4.4 \times 10^7 \text{ N/m}^2$ for a natural rubber vulcanisate ⁽¹¹⁾ and $\sigma_b = 3 \times 10^7 \text{ N/m}^2$ for SBR rubber ⁽¹³⁾.

At Columbia University, New York, tensile tests were performed on similar materials ⁽⁹⁾. Up to dewetting the curves are similar, but thereafter rupture was found at much lower strains, obviously because specimens of another shape were used ^{*}) which gave more stress concentrations in the clamps than the type of dumb-bell used in our investigation. Therefore, a comparison of these results with ours had to be restricted to the dewetting phenomenon and was not extended to the ultimate rupture properties.

4.4. Dewetting.

The maximum in the stress-strain curve is ascribed to dewetting; it coincides with blanching of the specimen. Dewetting is the failure of the rubber around the particles, or breakage of bonds between rubber and particle. Vacuoles are formed and the volume of the specimen increases suddenly ⁽³⁾. If this process is due to a failure of the rubber, dewetting should have the same time and temperature dependence as failure of unfilled rubber. Therefore, we investigated the relation-

^{*}) The ratio of smallest to largest width, b_2/b_1 , was 3 in our, and 1.5 in Columbia's investigations.

ship between dewetting time t_d , deformation at dewetting ϵ_d , and stress-at-dewetting σ_d in the same way as was done for the rupture properties. For practical reasons it was assumed that the maximum in the stress-strain curve represents the breakage of this intergranular rubber, although this breaking goes on beyond the yield point. Because the most pronounced maxima were found for the highest filler concentrations, the investigation was restricted to these materials. Results are indicated by crosses in Figs 19 and 20. In the same diagram, broken lines, copied from Figs 16 and 17, are drawn, corresponding to specimen rupture. Also inserted are results from the literature, namely: dewetting maxima from tensile tests at high strain rates ⁽⁹⁾, and rupture stresses from tensile creep experiments ⁽⁸⁾. Upon studying Figs 19 and 20 it will be evident that the dewetting stress, σ_d , depends in the same way on the reduced rupture time as the breaking stress, σ_b , for an unfilled material; apart from the dewetting stresses of the 45% filled materials being a factor of 4 lower than the breaking stresses of the unfilled material. The same holds for the deformation which appears to be a factor of 20 lower than for the unfilled rubber. These differences can easily be understood, because the strain in the rubber between the particles is much greater than the macroscopic strain. T.L. Smith ⁽¹⁷⁾ derived an expression for the ratio of yield and rupture strain:

$$\epsilon_d/\epsilon_b = 1 - 1.105 c^{1/3} \quad (6)$$

in which c denotes the volume fraction of the filler; at $c = 45\%$ this equation predicts a factor of about 0.15, which is not in contradiction with our findings.

We conclude: because the dewetting phenomenon depends on time and temperature in the same way as do the ultimate properties of the rubber matrix, we are very probably concerned with a process of failure in the rubber itself rather than a failure of bonds between rubber and particle.

Independent evidence for this viewpoint was obtained from microscopic observations of separate dewetted salt-particles fallen from the broken specimen. When water was added, it was seen that the salt particle dissolved but that some insoluble pieces remained, apparently pieces of rubber, which originally adhered to the surface of the salt crystal. Only part of the surface appeared to be covered with rubber. This investigation is still in progress.

Oberth and Bruenner⁽¹⁸⁾ came to the same conclusion, when they subjected polyurethane specimens in which a single steel ball of 3 mm diameter was imbedded to tensile tests: the rubber is the determining factor in the dewetting phenomenon.

4.5. Comparison with creep experiments performed previously.

Tensile creep experiments, up to failure, on filled rubbers were reported in Technical Report no. 5⁽⁸⁾. In a creep test, the specimen is subjected to a constant tensile force, which means that the stress is constant or slightly increasing during the test. In a stress-strain test, the strain rate is practically constant so that the stress may vary and exhibit the maximum in the stress mentioned earlier. For a creep test the configuration after dewetting is more or less unstable, resulting in a sharp increase in strain rate after dewetting.

From Fig. 5 it follows that the largest stress for a highly filled material is the dewetting stress; a creep test with this material consequently measures the dewetting stress. For lower filled materials the highest stress is the stress-at-break, as can be seen from Figs 2, 3 & 4. This is the same stress which is found in the creep experiment. This distinction is not of much practical importance since (see Fig. 19) it is obvious that, after the time-reduction, σ_d and α_b fall on the same curve.

The results obtained from the creep measurements as reported earlier⁽⁸⁾ are inserted in Figs 19 and 20. The agreement is rather good despite the fact that the type of deformation in both experiments is different. Moreover it should be noted that specimen dimensions and shapes were different. Because the particle size was not small with respect to the cross section, shape influences are likely to appear.

5. CONCLUSIONS.

1. When the filler content of the filled polyurethane rubber increases from 0 to 45% by volume, the rupture stress decreases by a factor of 5 at low and by a factor of 2.5 at high temperatures; the rupture strain decreases by a factor of 2 to 10.
2. The theory of the failure envelope could be applied to the rupture properties.
3. The stress-strain curves of materials with 45% filler show a maximum at strains of about 20%. The maximum is explained by assuming dewetting of the particles in the matrix.
4. The dewetting maximum is temperature and strain-rate dependent, in the same way as the ultimate properties of the unfilled rubber. This lends support to the view that dewetting is a failure of the rubber between the filler particles, and not a failure of the bond between rubber and filler particles, nor a failure of the filler particles themselves.

6. REFERENCES.

1. F.R. Schwarzl Mechanical Properties of Highly Filled Elastomers, Technical Report No. 1, Central Laboratory TNO, Delft, July 1962.
2. F.R. Schwarzl Mechanical Properties of Highly Filled Elastomers II, Influence of particle size and content of filler on tensile properties and shear moduli, Technical Report No. 2, Central Laboratory TNO, Delft, April 1963.
3. F.R. Schwarzl Mechanical Properties of Highly Filled Elastomers III, Influence of particle size and content of filler on thermal expansion and bulk moduli, Technical Report No. 3, Central Laboratory TNO, Delft, June 1964.
4. F.R. Schwarzl, H.W. Bree and C.J. Nederveen Mechanical Properties of Highly Filled Elastomers I, Proc. 4th Int. Congr. Rheology (Providence, 1963), E.H. Lee (Ed.), Interscience/Wiley, N.Y. (1965) Vol. 3, 241-265.
5. C.W. van der Wal, H.W. Bree and F.R. Schwarzl Mechanical Properties of Highly Filled Elastomers II, J. Appl. Polymer Sci. 9 (1965) 2143-2166.
6. F.R. Schwarzl et al. On Mechanical Properties of Unfilled and Filled Elastomers, Proc. Fourth Symposium on Naval Structural Mechanics, A.C. Dringen, H. Lisowitz, S.L. Kok, J.N. Crowley, Editors, Pergamon Press 1967, New York pp 503-538.
7. H.W. Bree, F.R. Schwarzl and L.C.E. Struik Mechanical Properties of Highly Filled Elastomers IV, Influence of particle size and content of filler on tensile creep at large deformations, Technical Report No. 4, Central Laboratory TNO, Delft, July 1965.

8. L.C.E. Struik, H.W. Bree and F.R. Schwarzl Mechanical Properties of Highly Filled Elastomers V, Influence of filler characteristics on tensile creep at large deformations, on rupture properties and on tensile strain recovery, Technical Report No. 5, Central Laboratory TNO, Delft, April 1966.
9. T. Nicholas and A.M. Freudenthal The effect of Filler on the Mechanical Properties of an Elastomer at high strain rates. Technical Report No. 36, Columbia University, Department of Civil Engineering and Engineering Mechanics, New York, November 1966.
10. M.L. Williams, R.F. Landel and J.D. Ferry J. Amer. Chem. Soc. 77 (1955) 3701-3707.
11. T.L. Smith J. Applied Physics 35 (1964) 27-36.
12. T.L. Smith J. Polymer Science A1 (1963) 3597-3615.
13. J.C. Halpin J. Applied Physics 35 (1964) 3133-3141.
14. J.C. Halpin and F. Bueche J. Applied Physics 35 (1964) 3142-3149.
15. R.F. Landel and R.F. Fedors Rupture Amorphous Unfilled Polymers in "Fracture Processes in Polymeric Solids", Ed. E. Rosen Interscience, New York, 1964, pp 361-485.
16. F.R. Schwarzl in Houwink/Staverman, "Chemie und Technologie der Kunststoffe I, Akademische Verlagsgesellschaft Geest & Portig K.-G. Leipzig, 4. Aufl (1962) p. 672.
17. T.L. Smith Trans. Soc. Rheol. 3 (1959) 115-136.
18. A.E. Oberth and R.S. Brauner Trans. Soc. Rheol. 2 (1958) 165-185.

CAPTIONS TO FIGURES.

- Fig. 1 Shape and dimensions, in mm, of the specimens used for stress-strain testing.
- Fig. 2 Stress-strain diagrams of unfilled polyurethanes at different temperatures and strain rates as indicated.
- Fig. 3 Stress-strain diagrams of polyurethane rubber filled with 15 vol% of sodium chloride particles of 0.1 mm at different temperatures and strain rates as indicated.
- Fig. 4 Stress-strain diagrams of polyurethane rubber filled with 30 vol% of sodium chloride particles of 0.1 mm at different temperatures and strain rates as indicated.
- Fig. 5 Stress-strain diagrams of polyurethane rubber filled with 45 vol% of sodium chloride particles of 0.1 mm at different temperatures and strain rates as indicated.
- Fig. 6 Stress-strain diagrams of a polyurethane rubber filled with various amounts of sodium chloride particles of 0.1 mm at +30°C.
- Fig. 7 Stress-strain diagrams of a polyurethane rubber filled with various amounts of sodium chloride particles of 0.1 mm at 0°C.
- Fig. 8 Stress-strain diagrams of a polyurethane rubber filled with various amounts of sodium chloride particles of 0.1 mm at -20°C.
- Fig. 9 Stress-strain diagrams of a polyurethane rubber filled with various amounts of sodium chloride particles of 0.1 mm at -30°C.
- Fig. 10 Stress-strain diagrams of a polyurethane rubber filled with various amounts of sodium chloride particles of 0.1 mm at -35°C.
- Fig. 11 Stress-strain diagrams of a polyurethane rubber filled with various amounts of sodium chloride particles of 0.1 mm at -40°C.
- Fig. 12 Stress-strain diagrams of a polyurethane rubber filled with various amounts of sodium chloride particles of 0.1 mm at -45°C.

- Fig. 13 Young's modulus E as a function of temperature as found from various tests.
- Fig. 14 Time-temperature shift function a_T vs temperature for polyurethane rubbers filled with various amounts of NaCl. Reference temperature is -35°C . The drawn line is a curve calculated according to Eq.(4) with $c_1 = 27.6$ and $c_2 = 38^{\circ}\text{C}$.
- Fig. 15 Failure envelopes for polyurethane rubbers filled with 0, 15, 30 and 45 vol% of sodium chloride particles of 0.1 mm.
- Fig. 16 Same as Fig. 15, upper part of the curves.
- Fig. 17 Reduced rupture stress vs reduced rupture time for polyurethane rubbers filled with 0, 15, 30 and 45 vol% of sodium chloride particles of 0.1 mm.
- Fig. 18 Elongation at rupture vs. reduced rupture time for polyurethane rubbers, filled with 0, 15, 30 and 45 vol% of sodium chloride particles of 0.1 mm.
- Fig. 19 Diagram of reduced stresses as a function of reduced rupture time. Plotted are rupture stresses obtained from Fig. 17, and from creep experiments, as well as dewetting stresses.
- Fig. 20 Diagram of elongation vs. reduced rupture time. Plotted are elongation at rupture obtained from Fig. 18, and from creep experiments, as well as elongation at dewetting.

TABLE 1. COMPOSITION AND PROPERTIES OF NaCl-FILLED SAMPLES PREPARED.

1	2	3	4	5	6	7	8	9
batch no.	Composition prepolymer g/100 g polyether Desmophen 3600			filler content vol % NaCl		fraction no.	NaCl-filler particle size μm	swe (% vo chloro form
	TDI	TMP	DB	from ingre- dients	from d			
3600/283	19.6	4.0	4.0	—	—			400
3600/284	19.5	4.0	4.0	—	—			402
3600/286	19.6	4.0	2.5	—	—			404
3600/288	19.6	4.0	2.5	—	—			400
3600/289	19.6	4.0	2.5	—	—			401
3600/290	19.5	4.0	2.5	—	—			401
3600/315	19.6	4.0	3.4	29.3	29.8	4	90-105	365
3600/316	19.6	4.0	3.4	29.3	29.7			376
3600/317	19.6	4.0	3.4	29.3	29.8			375
3600/318	19.5	4.0	3.4	29.3	29.9			370
3600/319	19.6	4.0	3.4	29.3	29.7			390
3600/320	19.6	4.0	4.6	14.5	14.8			383
3600/321	19.5	4.0	4.6	14.5	14.8			379
3600/322	19.6	4.0	4.6	14.5	14.8			391
3600/323	19.5	4.0	4.6	14.5	14.8			385
3600/324	19.6	4.0	4.6	14.4	14.8			395
3600/325	19.5	4.0	4.6	14.5	14.9			400
3600/326	19.6	4.0	3.4	29.3	29.7			383
3600/327	19.6	4.0	2.6	44.4	45.0			386
3600/328	19.5	4.0	2.6	44.4	45.2			393
3600/329	19.6	4.0	2.6	44.4	45.0			396
3600/330	19.6	4.0	2.6	44.4	45.2			392
3600/331	19.5	4.0	2.6	44.3	45.1			394
3600/332	19.5	4.0	2.6	44.3	45.2			398

A

7	8	9	10	11	12
action no.	NaCl-filler particle size μm	swelling 23°C (% vol.increase)		d (g/cm^3) 20°C	temperature of test °C
		chloro- form	trichloro- ethylene		
4	90-105	400	306	1.067	+30
		402	306	1.067	+30
		404	305	1.067	+30
		400	310	1.067	0, +30
		401	305	1.067	-45, -40, -35, -30, -20, +30
		401	307	1.067	+30
		365	287	1.398	-30, -20, +30
		376	289	1.397	-40, 0, +30
		375	285	1.398	-45, -35, +30
		370	285	1.399	+30
		390	290	1.397	+30
		383	295	1.235	+30
		379	289	1.235	+30
		391	300	1.236	+30
		385	299	1.235	-45, -35, +30
		395	302	1.236	-40, 0, +30
		400	304	1.237	-30, -20, +30
		383	297	1.397	+30
		386	290	1.563	+30
		393	291	1.565	+30
396	292	1.563	+30		
392	297	1.566	-45, -35, +30		
394	297	1.564	-45, -40, -30, -20, 0, +30		
398	299	1.566	-20, +30		

B

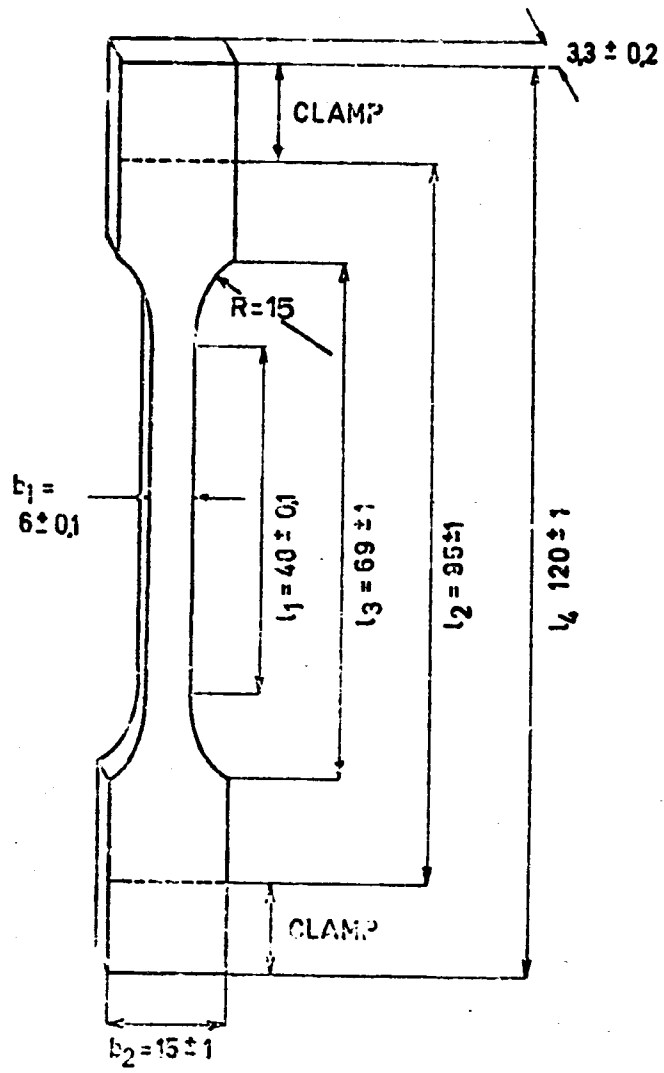
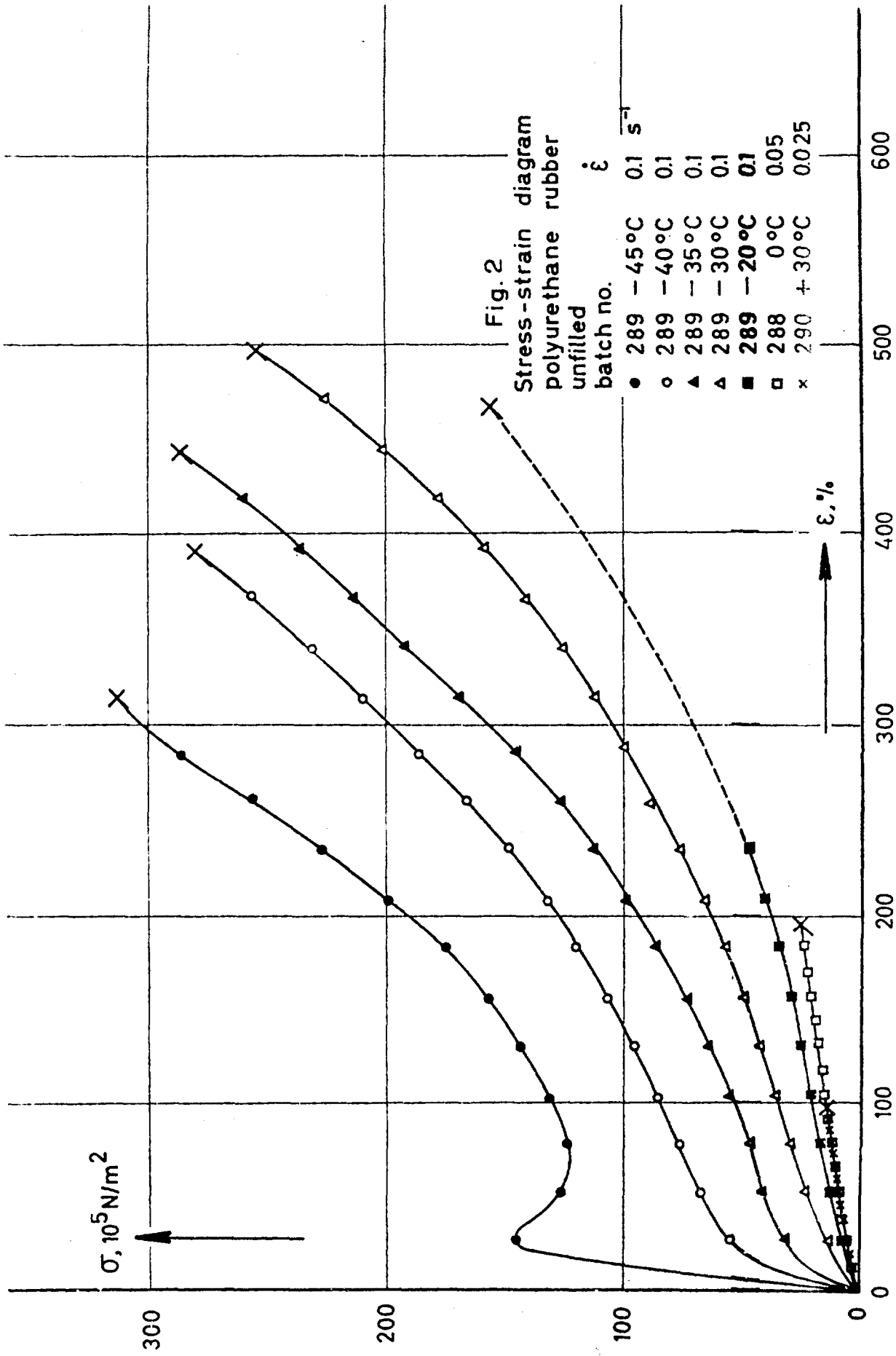


Fig. 1



$\sigma, 10^5 \text{ N/m}^2$

300

200

100

0

$\epsilon, \%$

0

100

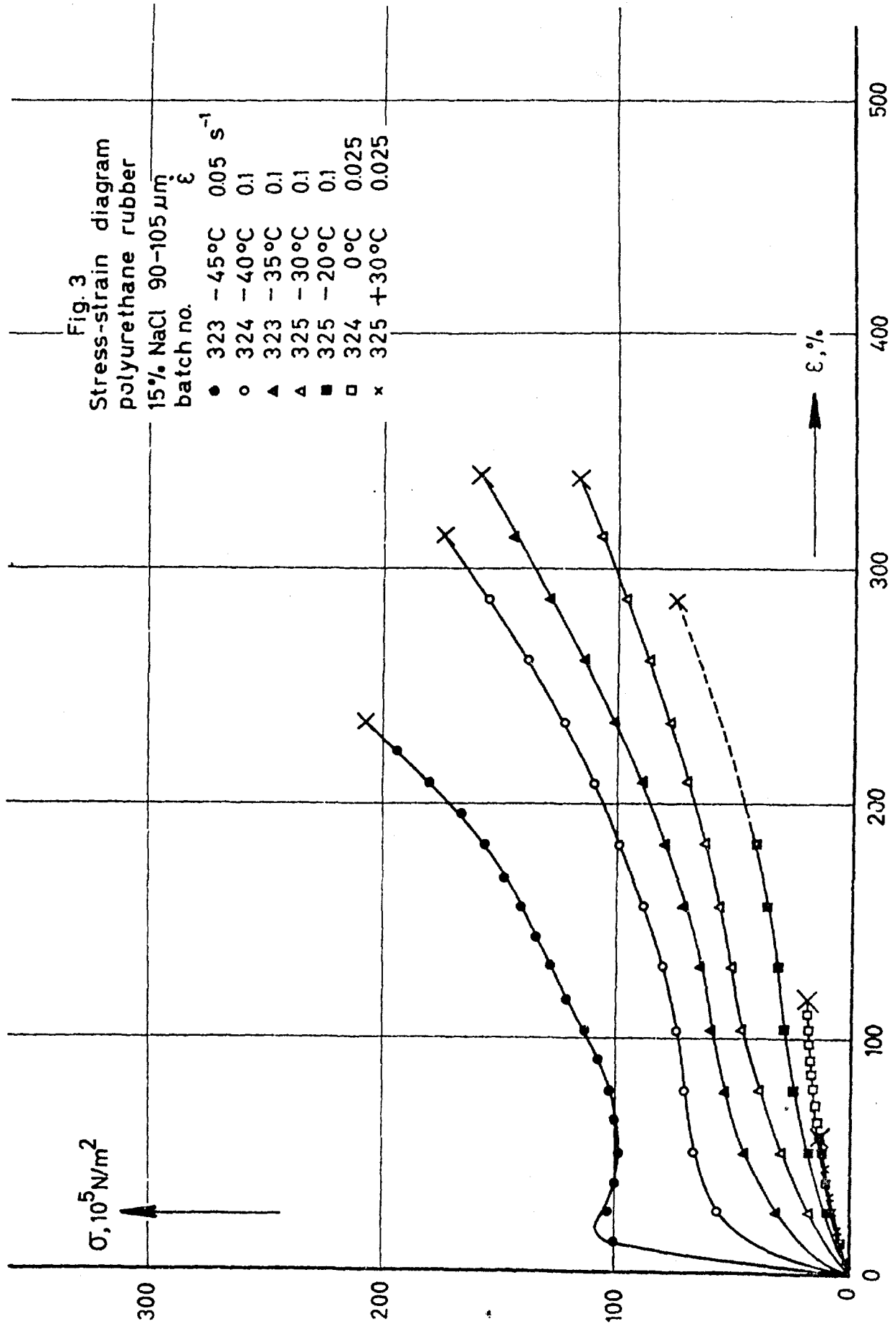
200

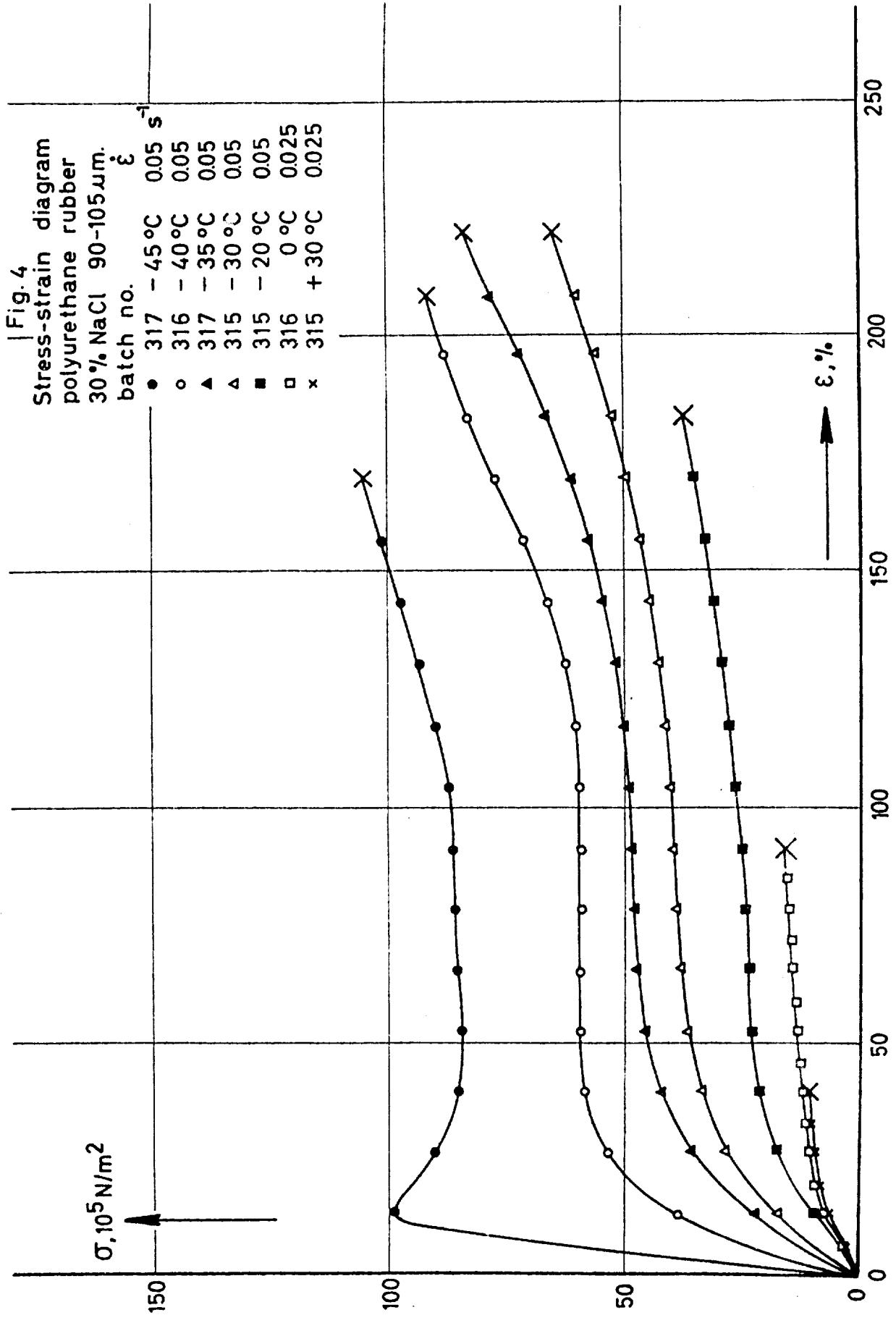
300

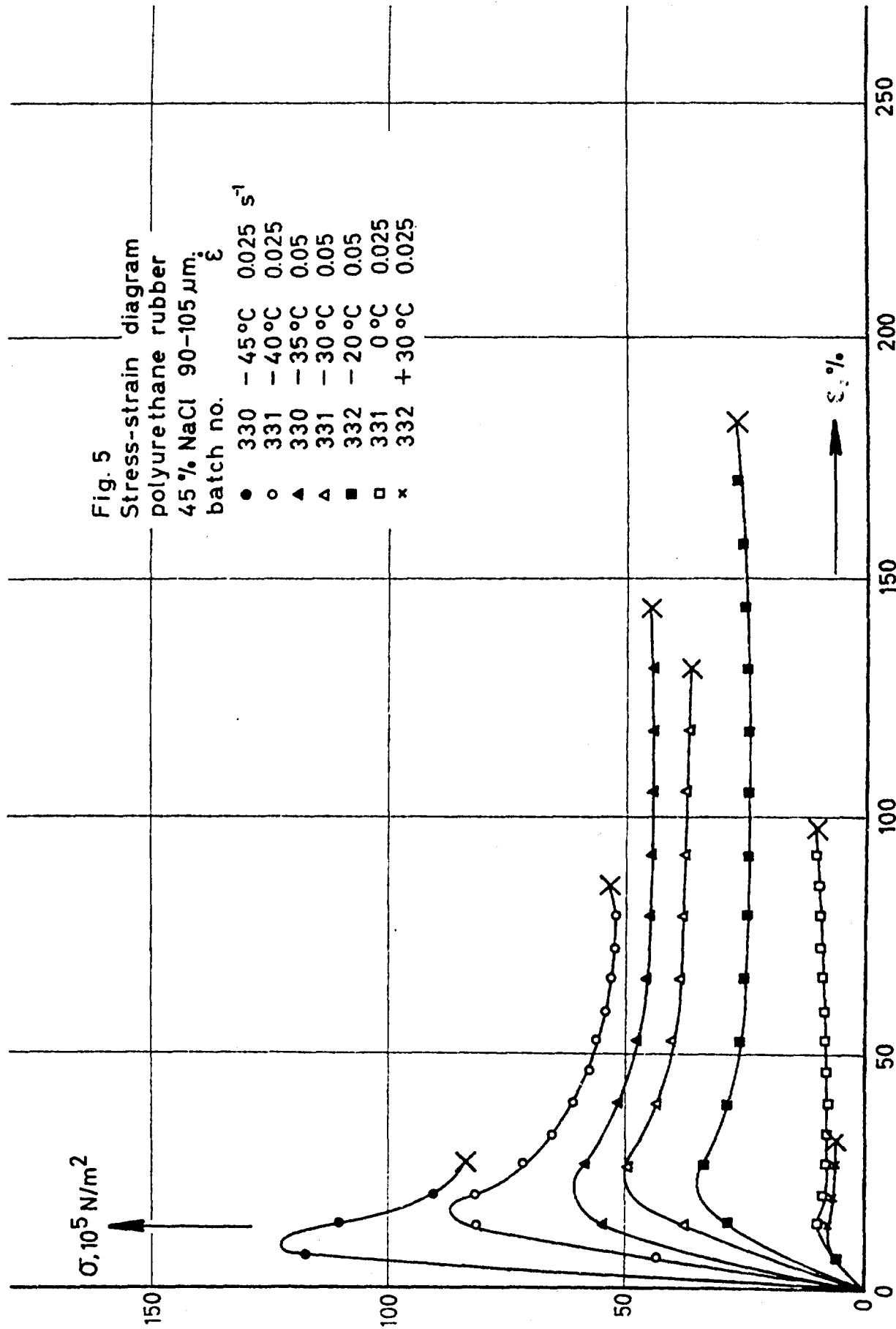
400

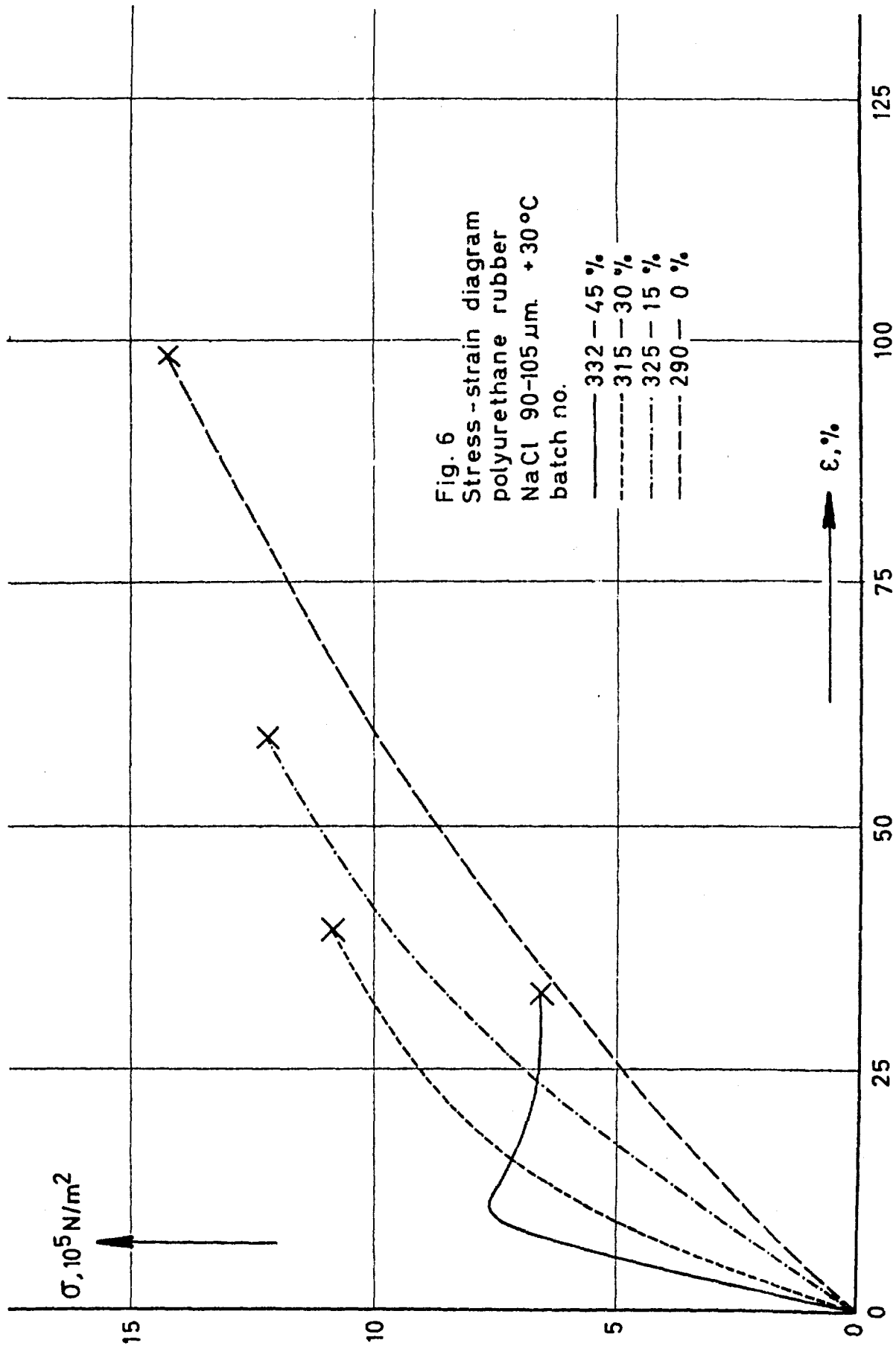
500

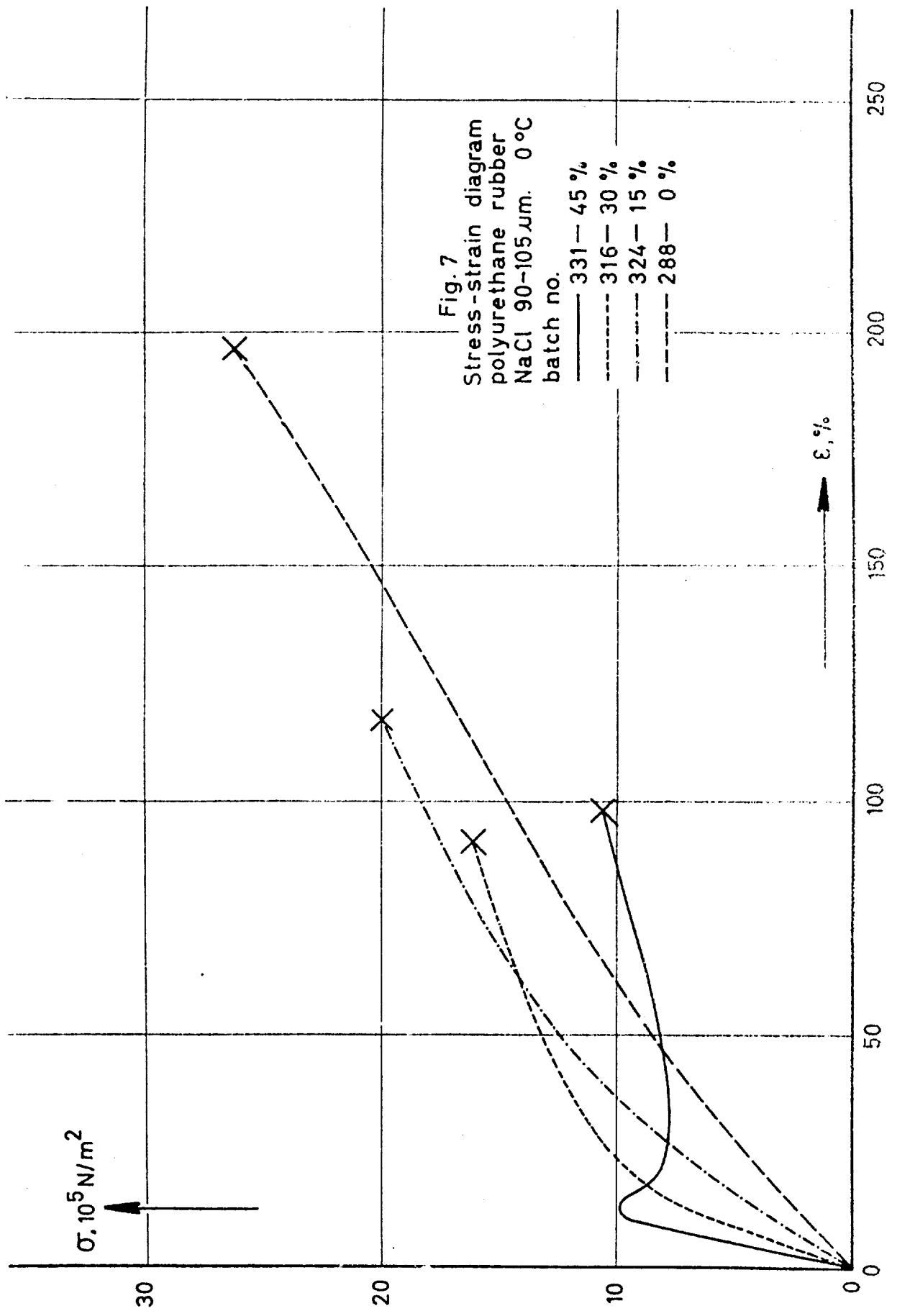
600

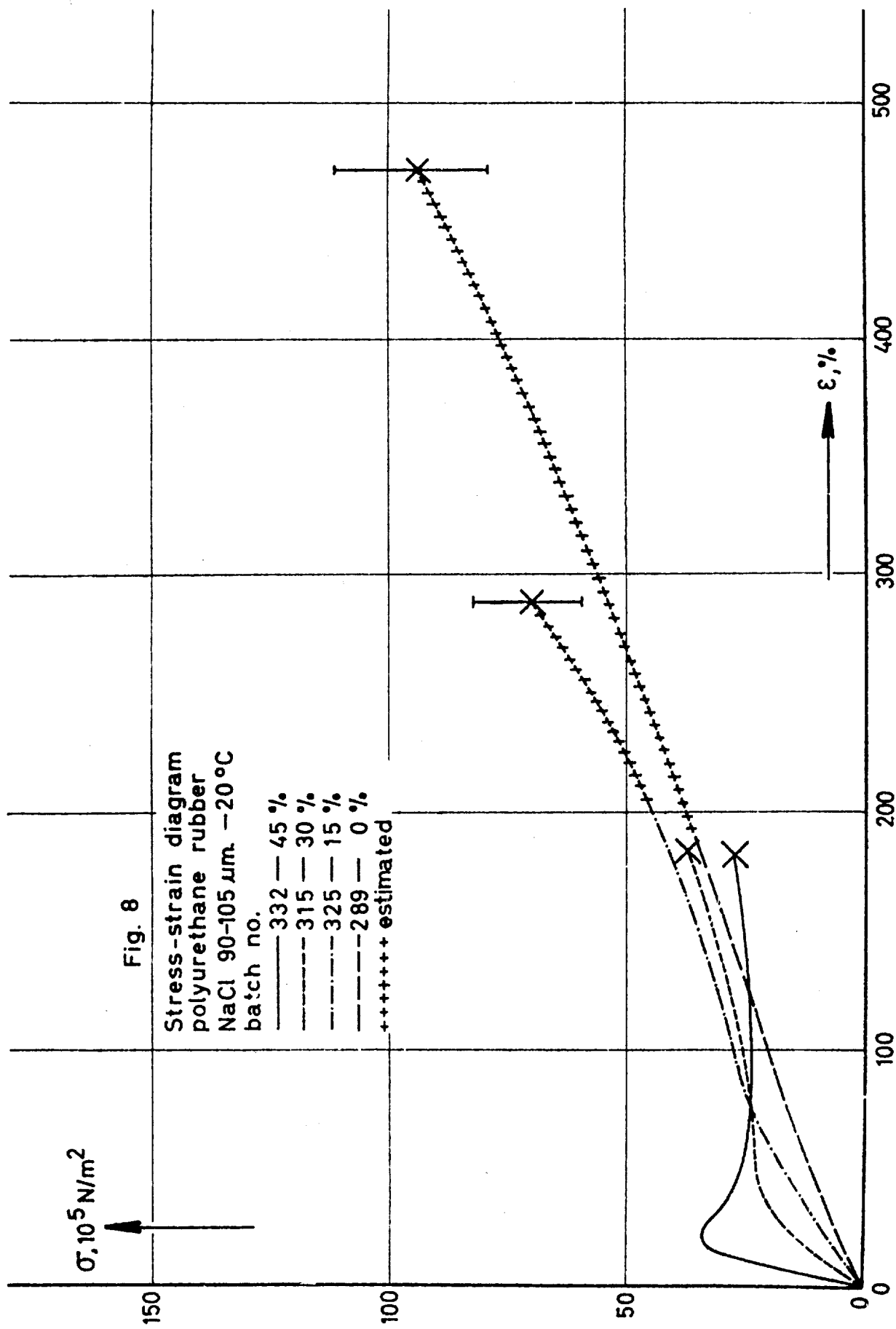


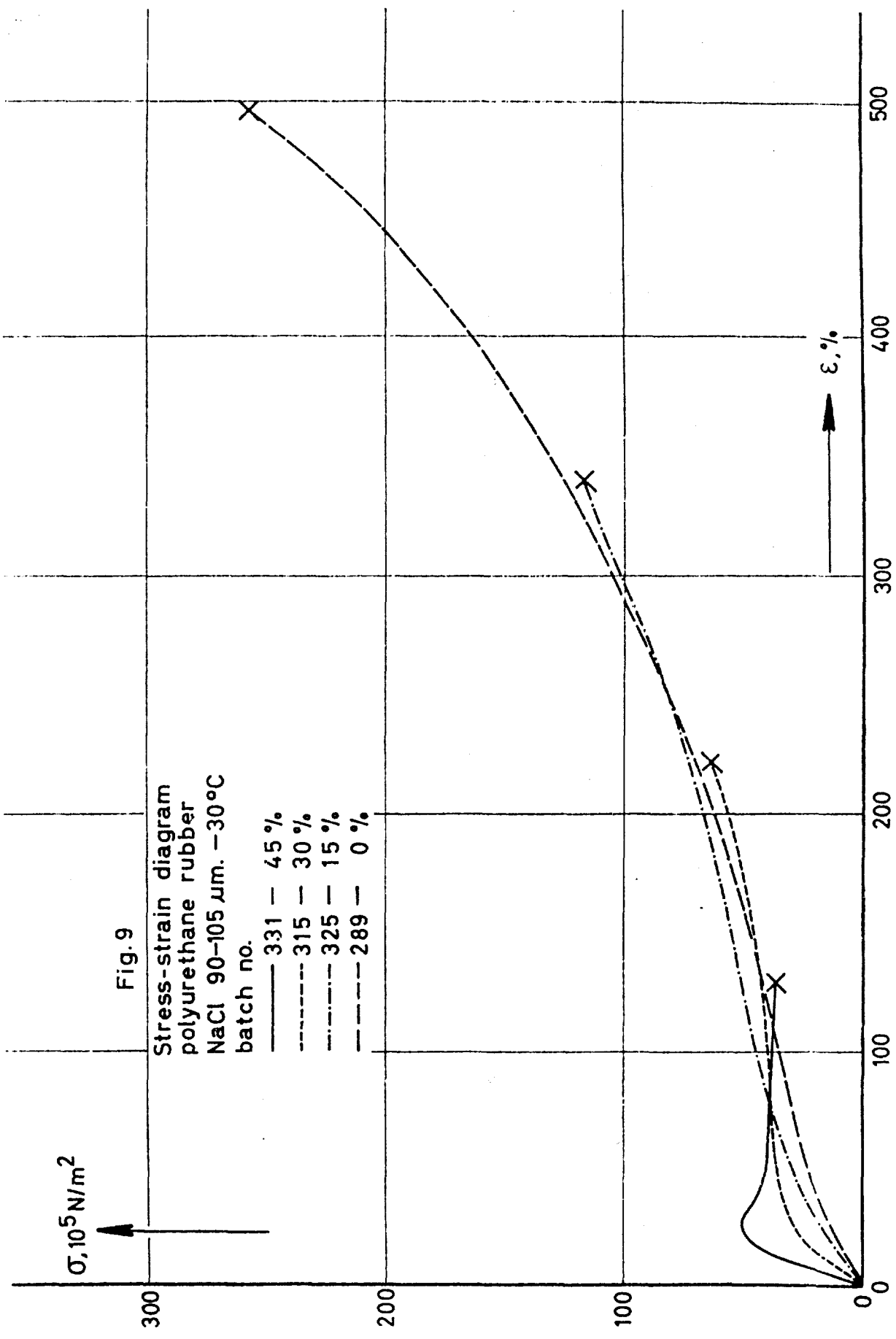


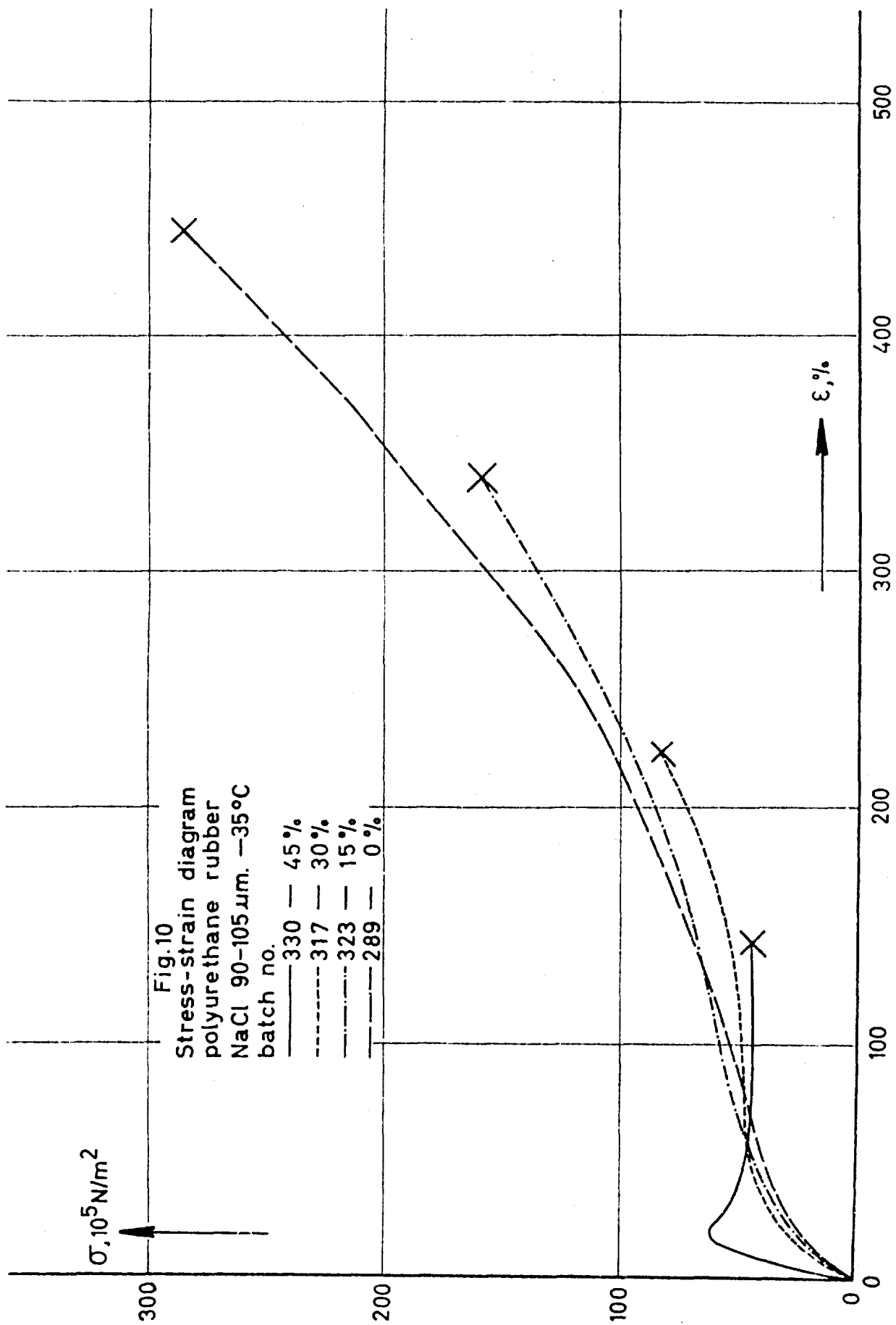


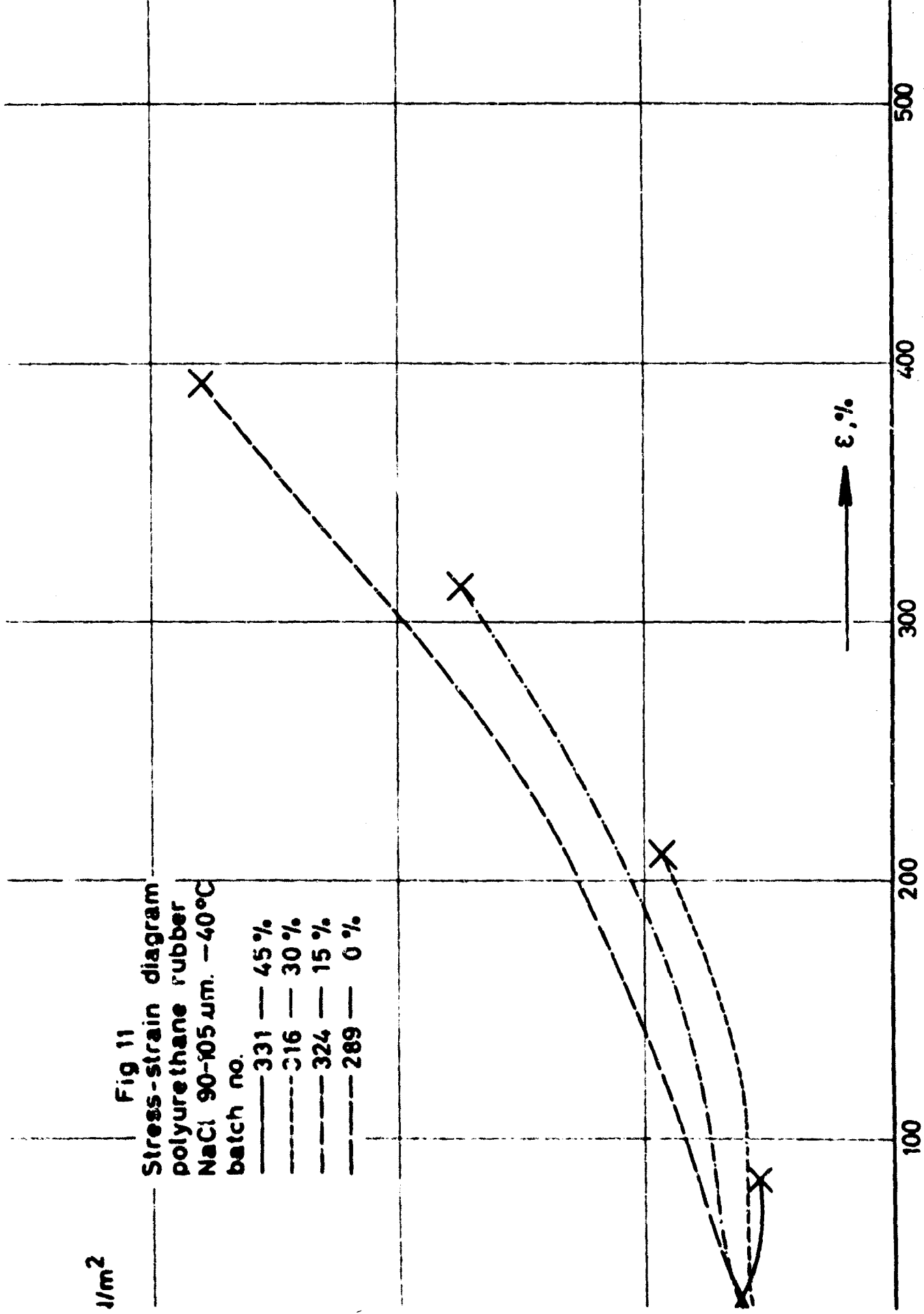


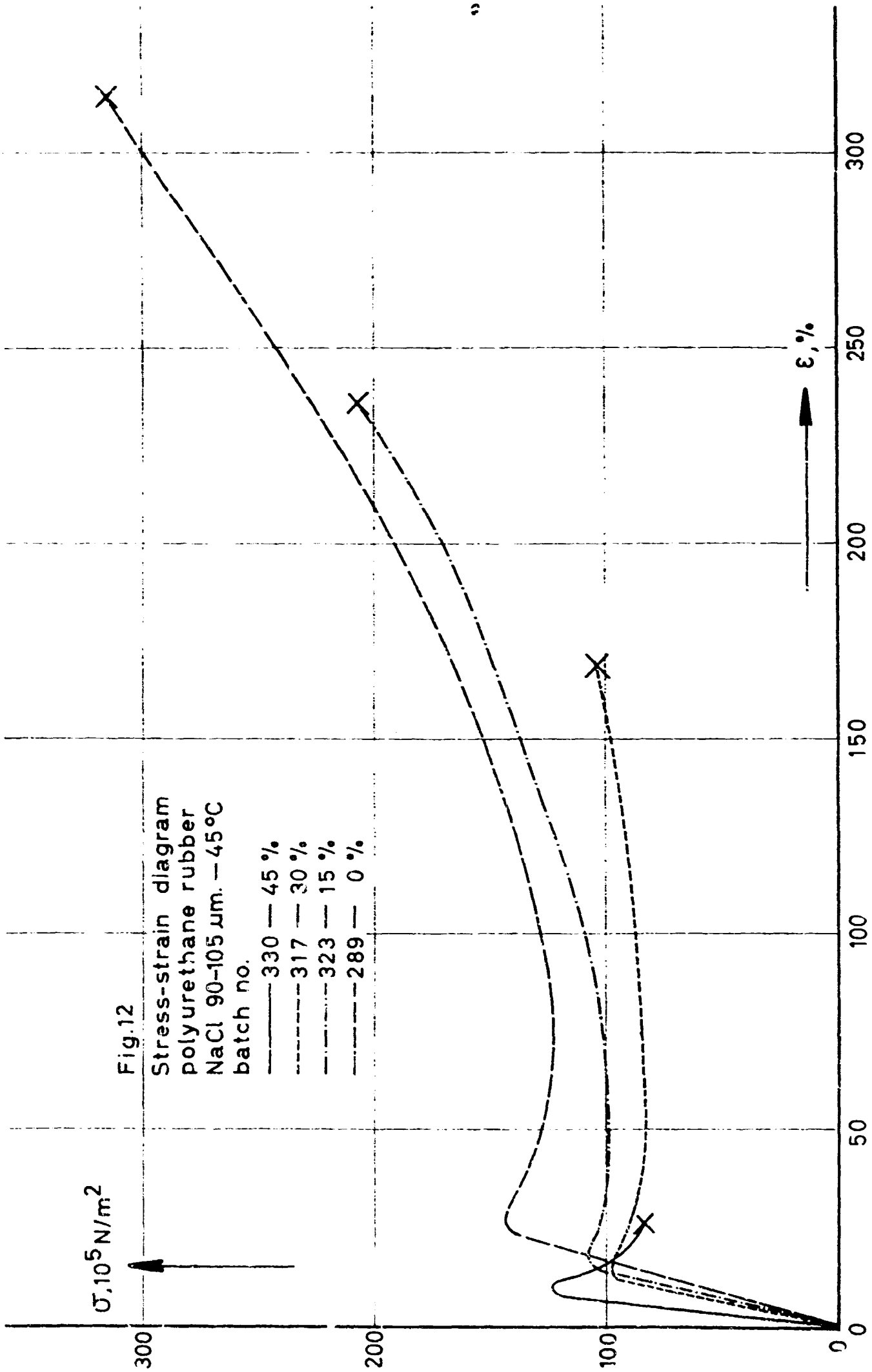












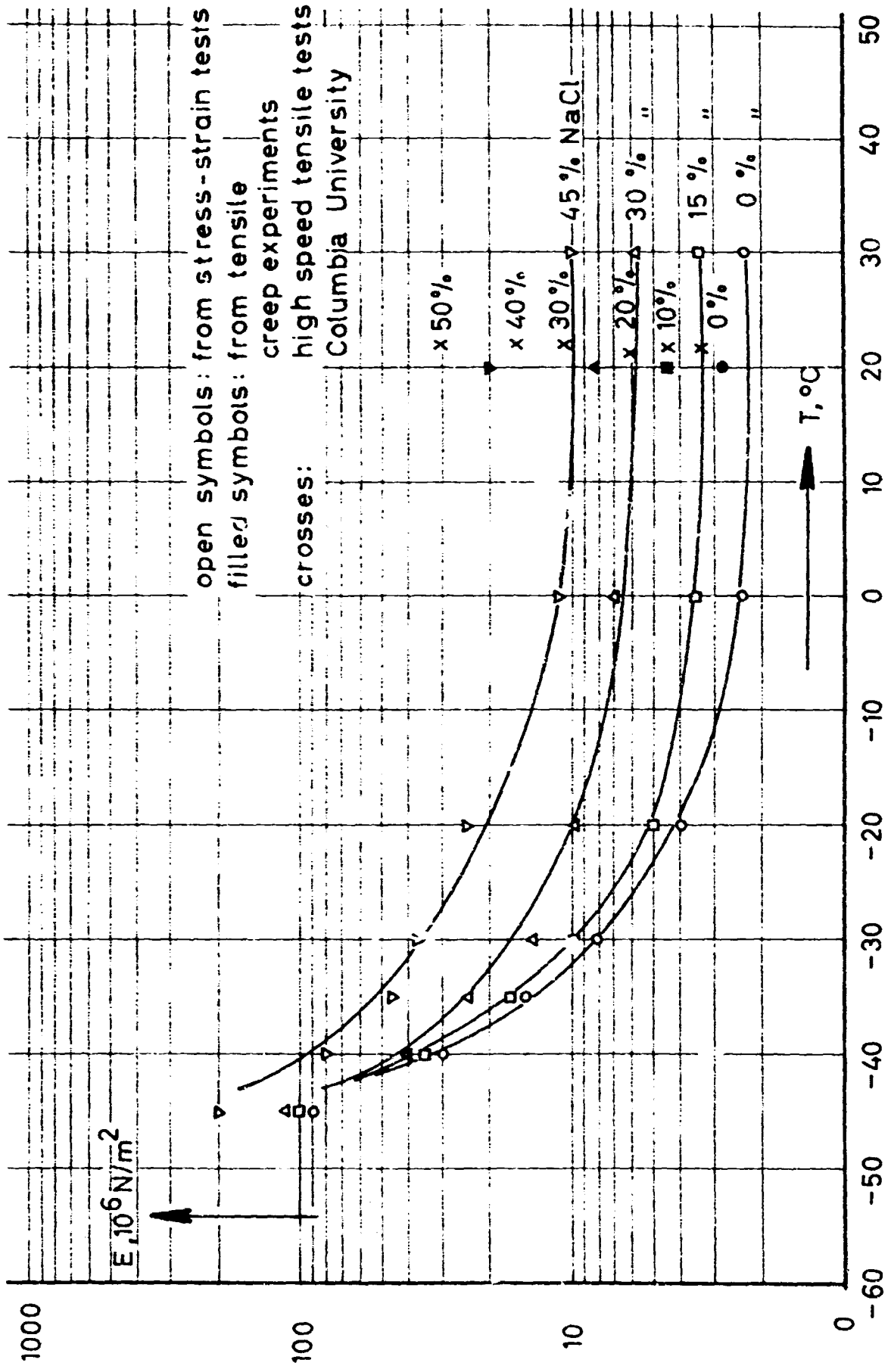


Fig.13

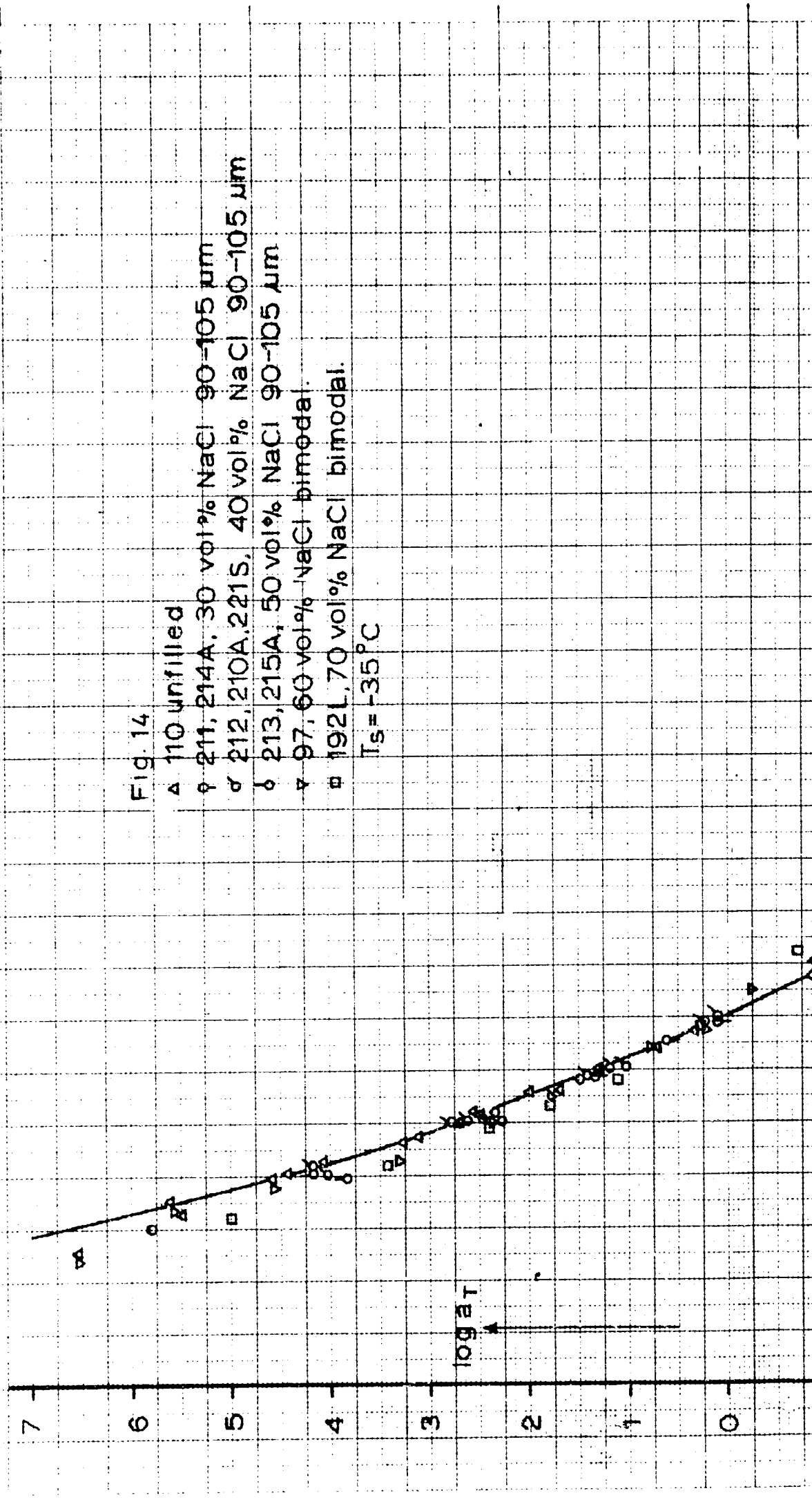
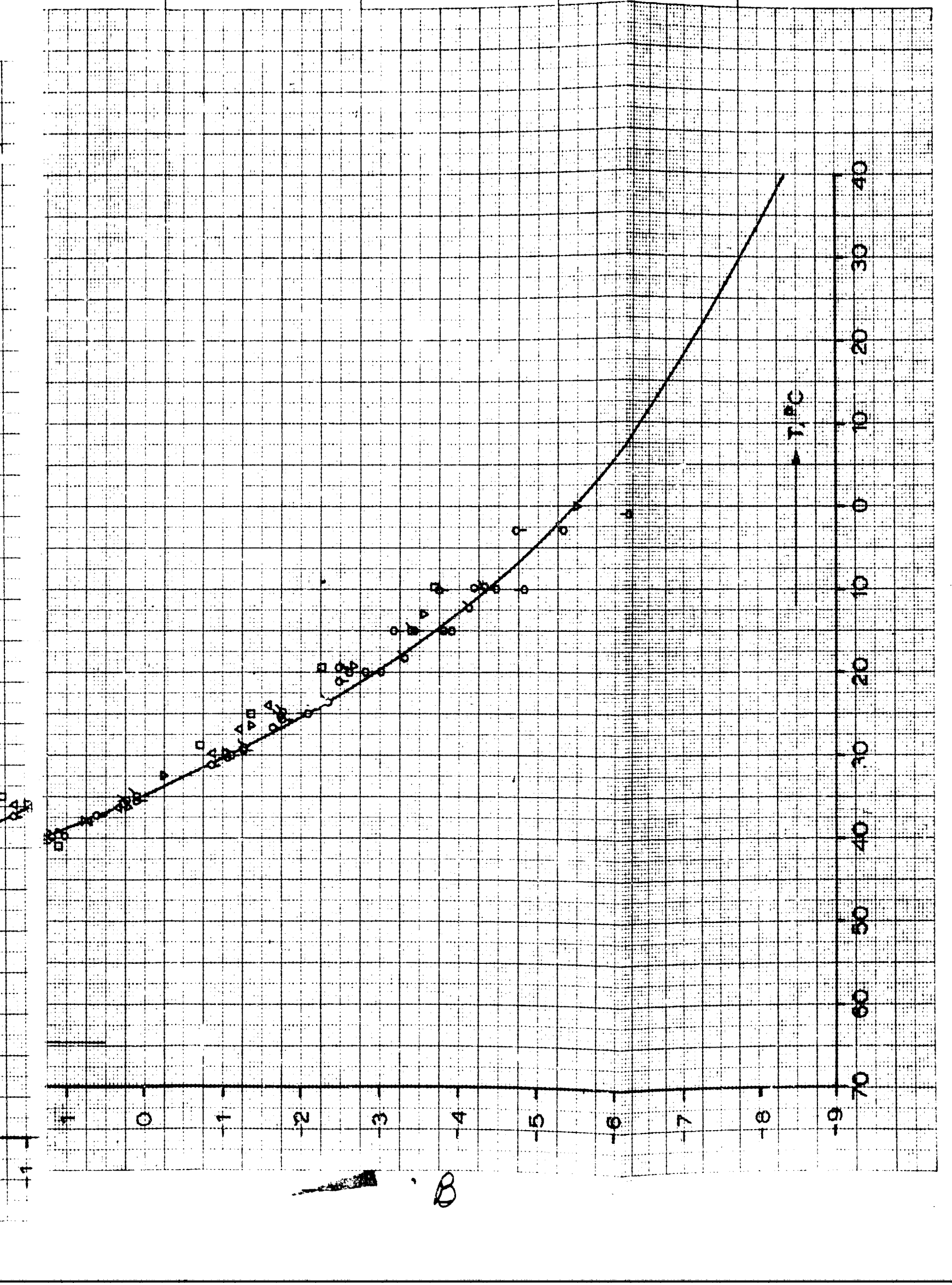


Fig. 14

- △ 110 unfilled
- 211, 214A, 30 vol% NaCl 90-105 μm
- 212, 210A, 221S, 40 vol% NaCl 90-105 μm
- ◇ 213, 215A, 50 vol% NaCl 90-105 μm
- ▽ 97, 60 vol% NaCl bimodal
- ▣ 192L, 70 vol% NaCl bimodal

$T_s = -35^\circ\text{C}$



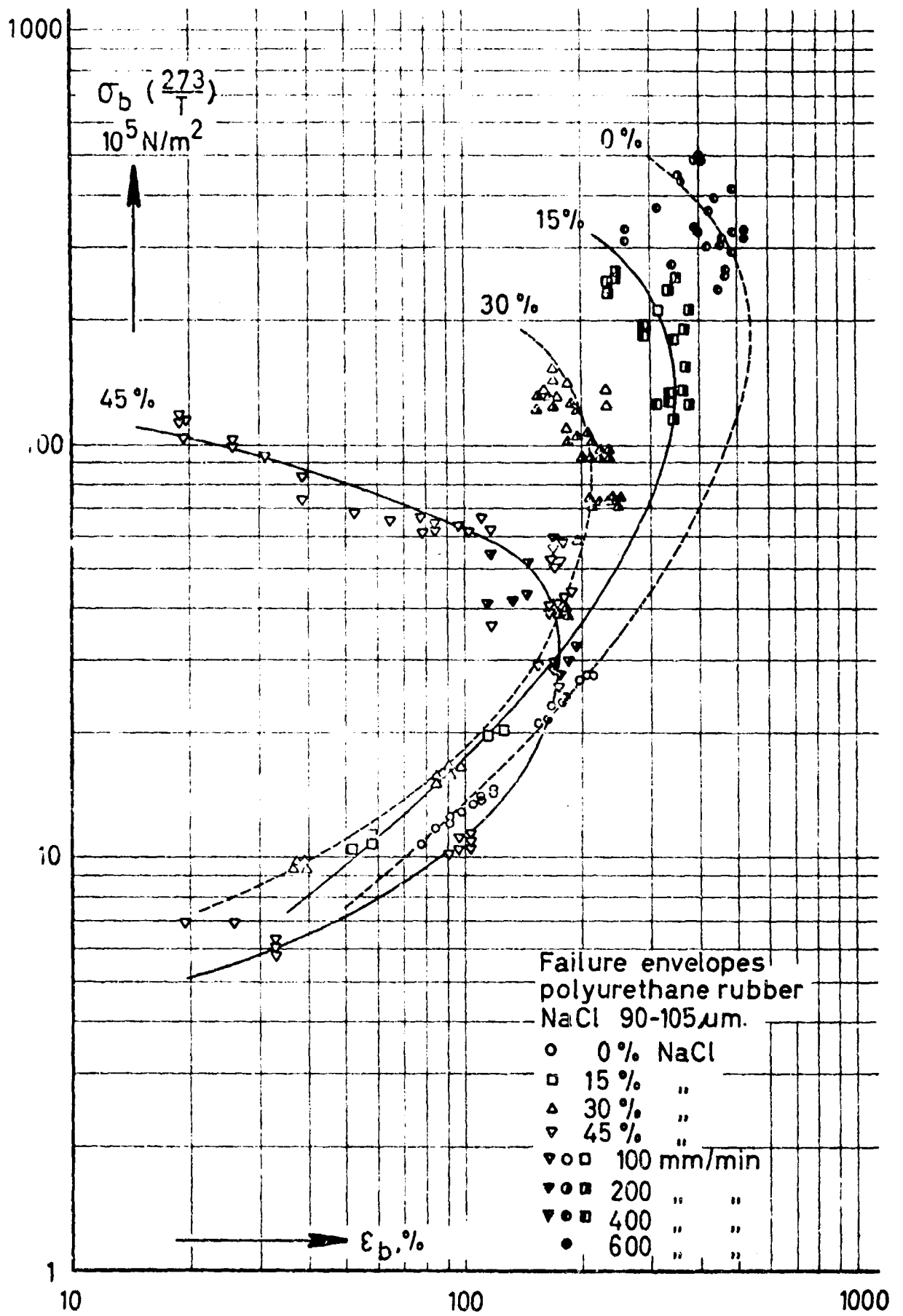


Fig.15

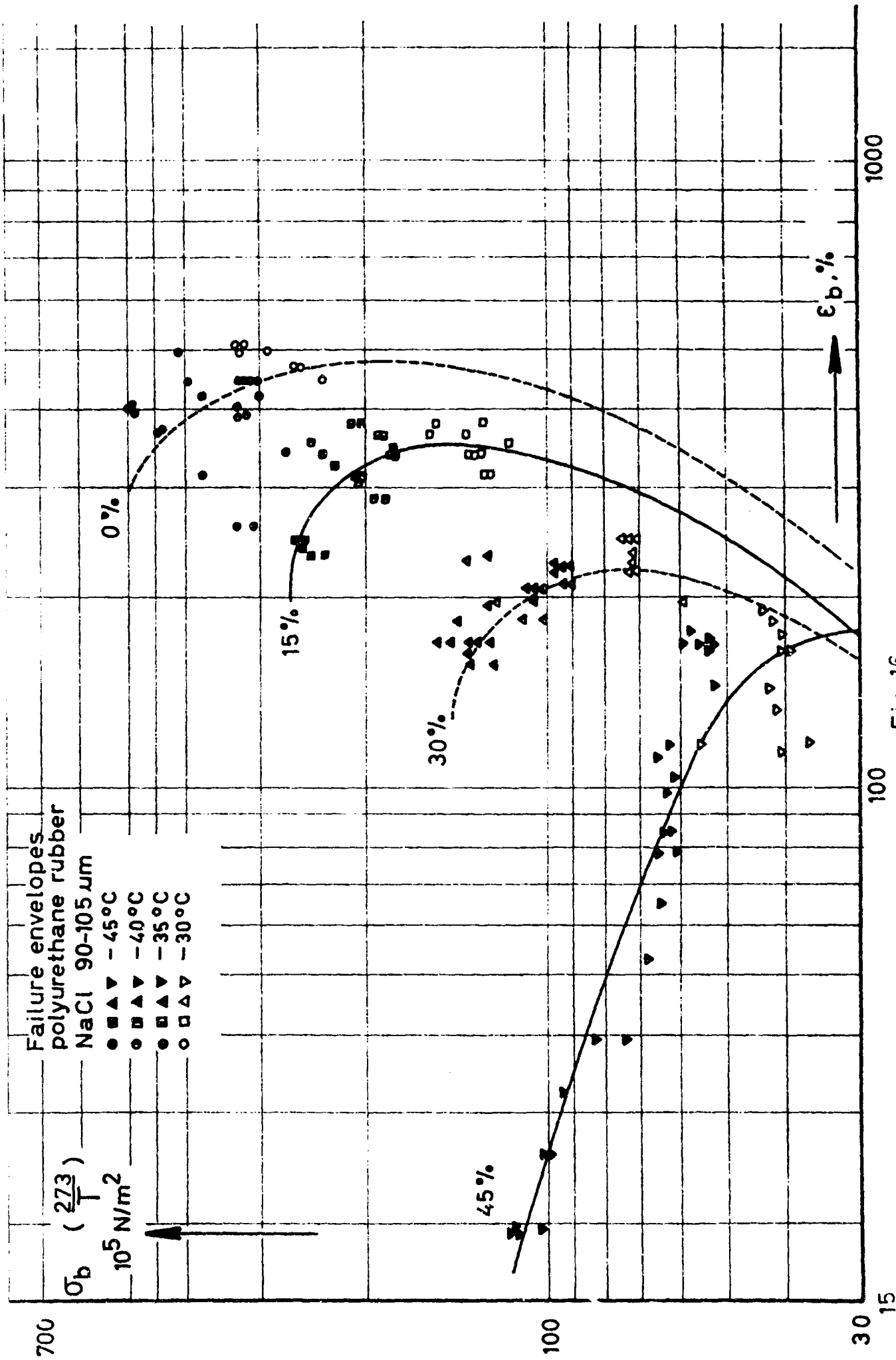


Fig. 16

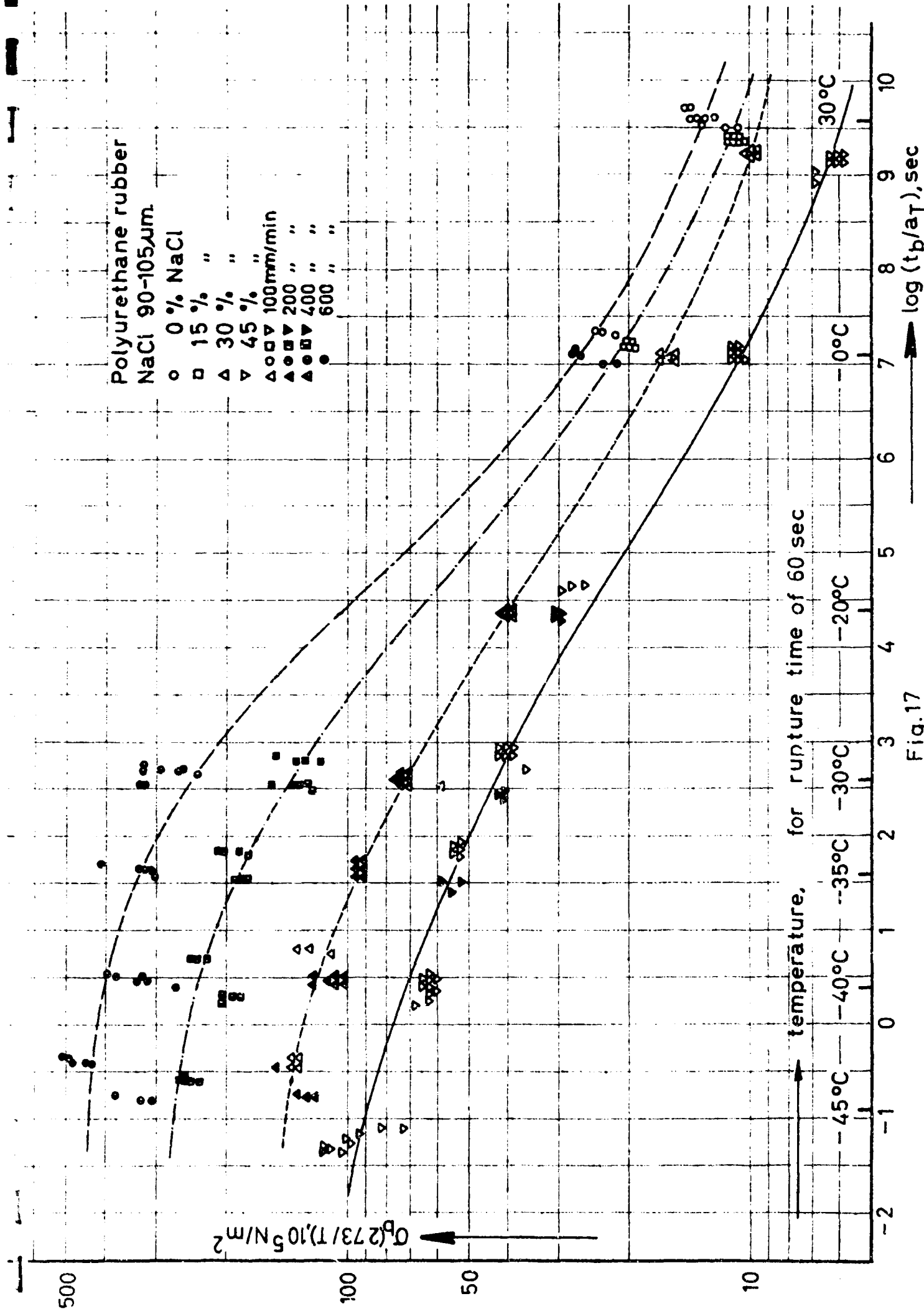


Fig.17

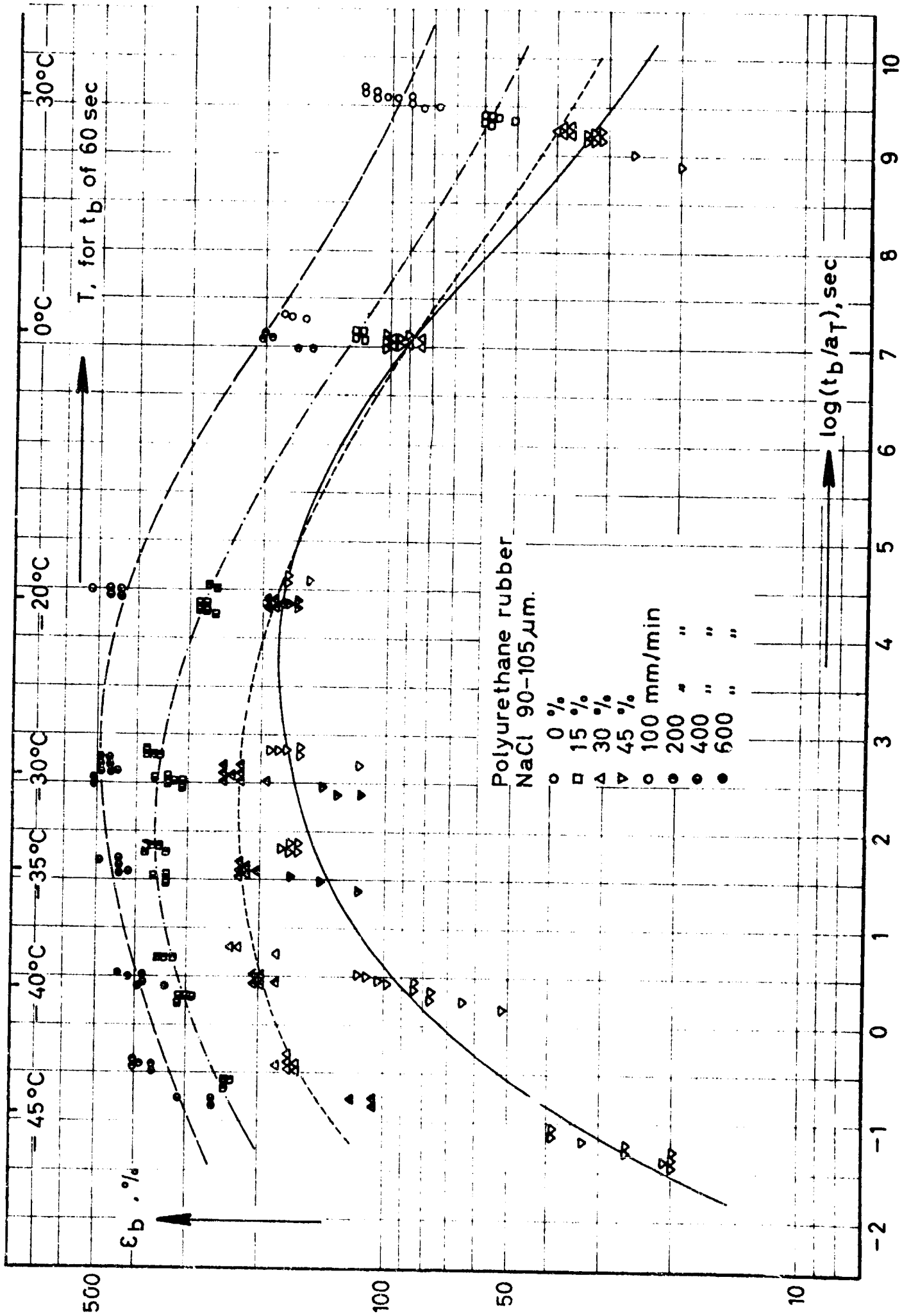
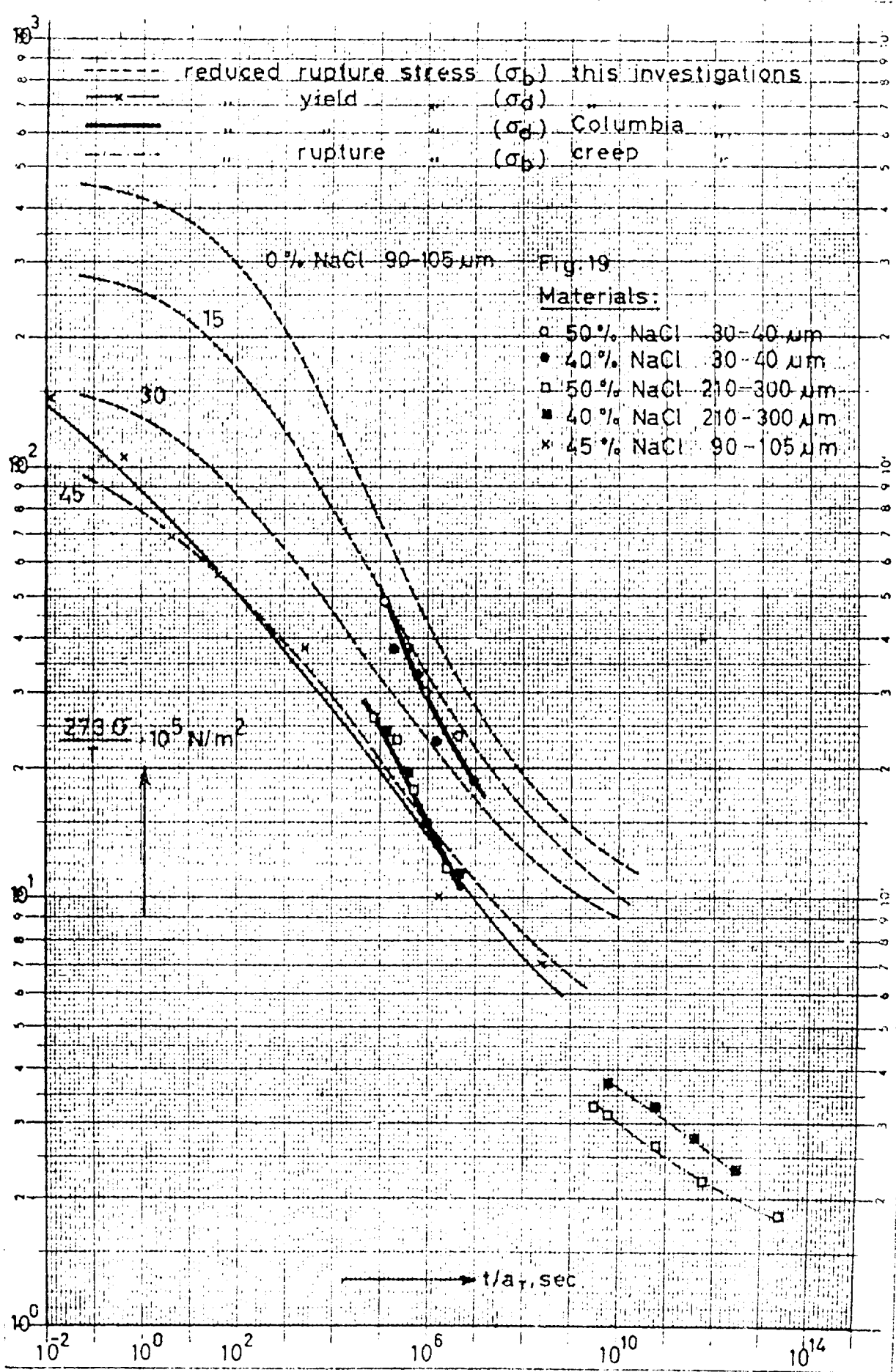


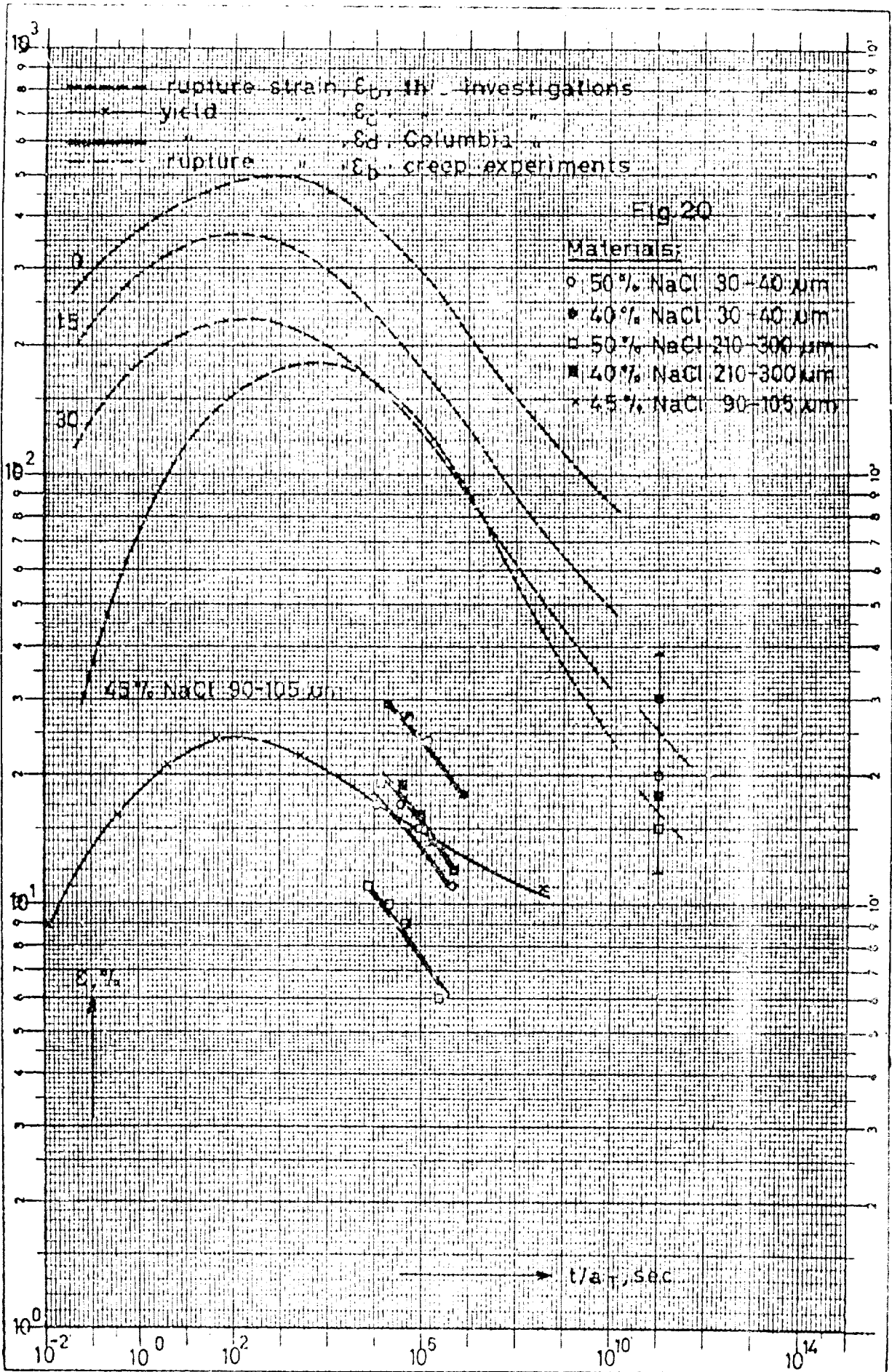
Fig. 18



X-axis log scale 1:10' Enkel 90 μm Yes, verdeckt in nr

No. 17

NY Drukery, Mercurus, Warmreer



X-axis log scale 1:10¹⁶ Ecmoid 90 mm. Y-axis scale in mm.

Fig. 17

M.V. Drobinskii, M. G. Mironovskii, V. M. Kargin

Unclassified

Security Classification

DOCUMENT CONTROL DATA - R & D

(Security classification of title, body of abstract and indexing annotation must be entered when the overall report is classified)

1. ORIGINATING ACTIVITY (Corporate author) Central Laboratory TNO - Delft Netherlands		2a. REPORT SECURITY CLASSIFICATION Unclassified	
		2b. GROUP	
3. REPORT TITLE Mechanical Properties of Highly Filled Elastomers VI. Influence of filler content and temperature on ultimate tensile properties.			
4. DESCRIPTIVE NOTES (Type of report and, inclusive dates) Technical Report no. 6			
5. AUTHOR(S) (First name, middle initial, last name) Nederveen, Cornelius J. Eree, Hendricus W.			
6. REPORT DATE June 1967	7a. TOTAL NO. OF PAGES 20	7b. NO. OF REFS 13	
8a. CONTRACT OR GRANT NO. N 62558	9a. ORIGINATOR'S REPORT NUMBER(S) Technical Report no. 6		
b. PROJECT NO. 4375	9b. OTHER REPORT NO(S) (Any other numbers that may be assigned this report) CL 67/34		
c.			
d.			
10. DISTRIBUTION STATEMENT Distribution list for unclassified technical reports.			
11. SUPPLEMENTARY NOTES		12. SPONSORING MILITARY ACTIVITY Office of Naval Research	
13. ABSTRACT <p>Results are presented of stress-strain tests performed at various temperatures and strain rates on materials filled with various amounts of sodium chloride particles with a mean size of 0.1 μm. Stress and strain at rupture decreased with increasing filler content. For each material investigated it was possible to construct the well-known failure envelope by means of which the results could be described adequately.</p> <p>The dewetting of the particles in the rubbery matrix, sometimes resulting in a maximum in the stress-strain curve, is ascribed to failure of the rubber between the particles and not to failure of the rubber-salt bond, because the dewetting maximum was dependent on temperature and time in the same way as the rupture properties of the unfilled material.</p> <p>The results are compared with earlier investigations, e.g. high speed tensile tests and creep experiments, and a good agreement is found.</p>			

Unclassified

Security Classification

14. KEY WORDS	LINK A		LINK B		LINK C	
	ROLE	WT	ROLE	WT	ROLE	WT
Polyurethane rubber Dummy propellant Filler content Rupture stress Elongation at rupture Failure envelope Reinforcement Vacuoles Dewetting						

DD FORM 1473 (BACK)

Unclassified

Security Classification

4-31409